EXPERIMENTAL INVESTIGATION FOR THE EFFECT OF THE CORE LENGTH ON THE OPTIMUM ACID FLUX IN CARBONATE ACIDIZING

A Thesis

by

KAI DONG

Submitted to the Office of Graduate Studies of
Texas A&M University
in partial fulfillment of the requirements for the degree of

MASTER OF SCIENCE

August 2012

Major Subject: Petroleum Engineering

Experimental Investigation for the Effect of the Core Length on the

Optimum Acid Flux in Carbonate Acidizing

EXPERIMENTAL INVESTIGATION FOR THE EFFECT OF THE CORE LENGTH ON THE OPTIMUM ACID FLUX IN CARBONATE ACIDIZING

A Thesis

by

KAI DONG

Submitted to the Office of Graduate Studies of
Texas A&M University
in partial fulfillment of the requirements for the degree of

MASTER OF SCIENCE

Approved by:

Co-Chairs of Committee,	Ding Zhu
	A. Daniel Hill
Committee Member,	Yuefeng Sun
Head of Department,	A. Daniel Hill

August 2012

Major Subject: Petroleum Engineering

ABSTRACT

Experimental Investigation for the Effect of the Core Length on the Optimum Acid Flux in Carbonate Acidizing. (August 2012)

Kai Dong, B.S., China University of Petroleum (Beijing)

Co-Chairs of Advisory Committee: Dr. Ding Zhu
Dr. A. Daniel Hill

Matrix acidizing is commonly used to stimulate wells in carbonate reservoirs. Large amounts of lab tests indicate an optimum acid interstitial velocity ($V_{i\text{-opt}}$, injection rate over flow area and porosity) exists, which results in the minimum volume of acid required for wormhole propagation and best stimulation results. Previous tests showed that the $V_{i\text{-opt}}$ increased with increasing core length, but it is not clear if the $V_{i\text{-opt}}$ can be independent of the core length when the core length reaches a certain value. In this work, a series of core flood experiments with different core lengths was carried out to determine the $V_{i\text{-opt}}$. Results showed that the $V_{i\text{-opt}}$ became a constant when the core length reached a certain length. The finding of this study can guide lab researchers to use proper core lengths when determining the $V_{i\text{-opt}}$.

DEDICATION

To my parents

ACKNOWLEDGEMENTS

I would like to thank my committee chair, Dr. Ding Zhu, and my committee members, Dr. Hill and Dr. Sun, for their guidance and support throughout this research. Thanks also to my friends who make my life full of fun in the past two years at Texas A&M University. I will always remember the days together with them.

Special thanks to Miss NT in China University of Petroleum (Beijing).

Thanks to my parents for their support and encouragement.

I appreciate all the undertakings around me, which made me more mature and confident.

The places I have always been are important in my life. The Richardson Building of the Harold Vance Department of Petroleum Engineering, Office #714, is my working place. Arbor Square apartment is my living place. I like all the places such as Student Recreational Center, Reed Building basketball court, Evans Library and Poor Yorick's Café, Cinemark, Grand Station, HEB and Chef Cao's.

Additionally, I would like to acknowledge the financial support from Middle East Carbonate Stimulation joint industry project, as well as the facility support of the Harold Vance Department of Petroleum Engineering.

NOMENCLATURE

A	Core Cross-sectional Area, cm^2
L	Core Length, cm
d	Core Diameter, cm
V	Volume, cm^3
M	Core Mass, g
ρ	Density, g/cm^3
ϕ	Porosity, dimensionless
C	Concentration
q	Injection Rate
t	Acid Injection Time
V_i	Interstitial Velocity

TABLE OF CONTENTS

Page

LIST OF FIGURES

FIGURE Page

FIGURE Page

LIST OF TABLES

1. INTRODUCTION

1.1 Problem Statement

Carbonate acidizing technique is widely used to stimulate wells in carbonate reservoirs. The acid is injected from the surface to the formation and creates long flow channels called wormholes that can bypass damaged zones around the well. A lot of work has been published to study this process, among which some work focuses on the acid-injection-rate selection. Lab results have indicated that an optimum acid injection rate exists, which results in the best stimulation result while using the least amounts of acid. Coreflood experiment is the most reliable way to get this optimum acid injection rate for different carbonate rocks. Field designs of acid treatments are based on the lab experimental observations to determine the acid injection rate and acid volume needed.

However, the core dimension can affect the experimental results. Under identical conditions, larger-diameter cores result in a lower optimum acid interstitial velocity ($V_{i\text{-opt}}$, injection rate over flow area and porosity), and longer cores results in a higher one. In order to get correct experimental results, we need to eliminate the core-size effect. If we only take the effect of core length into consideration, the problem comes to whether $V_{i\text{-opt}}$ is independent of the core length when the core length reaches a certain value. If so, the effect of core length would be eliminated so that the right core length can be selected in the lab.

This thesis follows the style of *SPE Journal*.

1.2 Background and Literature Review

Matrix acidizing in carbonate formation is a process of fluid-solid chemical reactions in porous medium, which is often accompanied by a continuous alteration of the pore structure of the medium. Highly conductive channels, referred as wormholes, are formed to bypass damaged zones around the wellbore, so that the reservoir fluid can be produced with minimum pressure drop. The wormhole structure is an important factor when evaluating the stimulation result.

For a long time, researchers have been looking for the wormhole formation mechanism and they have developed various models to simulate this process. Schechter and Gidley (1969) treated the pores as cylindrical tubes distributed randomly and studied how the pores are enlarged and how the pore distribution is changed due to surface reaction, and they also developed an evolution equation. The conclusions that they drew from the study are that the pores are enlarged by reaction and two pores can emerge as one larger pore by collision. It is the larger pores that determine the response of the system to acid injection. So the distribution of larger pores plays an important role. Guin et al (1971) conducted experiments to validate the pore evolution equation. They used the cold concentrated HF (-30 ºC) as a retarded acid, to react with the glass. Meanwhile, Guin and Schechter (1971)solved a pore evolution equation by Monte-Carlo method using a small sample of pore size distribution as initial condition, and they found that for a wide range of pore size distribution, the pore evolution equation gives approximately the same results, which indicates that for most cases, the designers do not necessarily need the initial pore size distribution to utilize their correlation. Based on

their work, wormholing can be explained by the collision mechanism, which is also an essential feature of the pore evolution model developed by Schechter, Gidley and Guin.

Schechter, Gidley and Guin's work help people to understand the basic physics of wormholing from pore scale. Wormholing was treated as stochastic process and stochastic models were developed. There is similarity between wormholing process and viscous fingering of two fluids displacement. Viscous fingering occurs as a result of a sharp increase of mobility when a small perturbation appears at the interface between the fluids; while at the wormhole front, mobility ratio also increases sharply due to the sharp permeability increases. Therefore, the method used in viscous fingering can be applied to wormholing. Nittmann et al. (1985) showed viscous fingering in Hele-Shaw Cell and tried to quantify this phenomenon. They found that viscous fingers are fractals and many different random structures have the identical value of the fractal dimensionality. Daccord et al. (1986) found for a wide range of shear thinning fluids, flow rates, and plate separations, radial viscous fingers have a fractal dimension same as diffusion limited aggregation (DLA). Their work provides a link between viscous fingering and DLA model. Based on the similarity between wormhole propagation and viscous fingering, DLA model may be applied to the research of wormholing. Daccord (1987) injected water to plaster to generate almost the same dissolution pattern as wormholes in acidizing. He then used the basic assumptions of the DLA model to develop his own model based on the real mechanism observed in his experiment. After analyzing the deficiency of previous stochastic models, Pichler et al. (1992) modified the DLA model and developed a permeability driven fingering model. He incorporated the permeability

heterogeneity, permeability anisotropy and natural fractures into his model. It gives the possibility to show the impact of different factors on the wormhole pattern. This model showed good promise for predicting wormhole propagation quantitatively.

Daccord et al. (1989) presented a wormhole propagation model based on the dissolution pattern created by injecting water into plaster. He quantified wormholes by a unique parameter, the equivalent hydraulic length. His model is based on the diffusion limited mechanism for acid transport to the rock surface, but does not take fluid loss into account, which plays an important role in wormhole growth. Besides, the dissolution pattern he used in his model comes from the water-plaster system, and this may not represent the wormhole pattern in carbonate acidizing properly. Therefore, Daccord's model should be used with caution (Economides, et al., 1993). In his work, Daccord concluded that for highly reactive systems, an optimum flow rate exists. This optimum flow rate becomes the basis for many following wormhole studies.

Hoefner and Fogler (1987) studied the influence of acid diffusivity on wormholing. The reason is in the field, aqueous HCl can only penetrate 1 to 3 ft of the formation, but acid emulsion can penetrate farther. Coreflood results show that the microemulsion can stimulate cores in fewer pore volumes than HCl. Besides, wormholes can break through the core under conditions of low injection rates where aqueous HCl fails completely. Their work help to better understand the diffusion effect during wormholing.

Hoefner and Fogler (1988) then further developed their research on coupling mechanism of acid convection and reaction, thus gave a deeper understanding of the

wormhole formation. Dolomite and limestone were used to show the results of different reaction rates. Convection was controlled directly by changing injection rate. Woods castings were made based on the acidized cores to show the wormhole structures under different flow rates. Analysis on those castings showed that the pore evolution process is controlled by the Damkohler number, which is the ratio of reaction over convection. They then stated the relative relationship between acid flow and dissolution in a clear way (Hoefner and Fogler, 1989). For a slow reaction rate like HCl with dolomite, if the convection rate is high, the dissolution will be branched, no wormholes will form. For a high reaction rate, such as limestone, if the convection rate is extremely high, we can say that the reaction rate is relatively low compared with convection rate. The case is the same as dolomite that dominant wormhole is unlikely to form. At average convection rate, reaction dominates the process and wormholes will form. They concluded that it is the ratio of reaction over convection, referred as Damkohler number, that determines the wormholing process and wormhole structure.

Besides the analysis based on the coreflood experiments and wormhole castings, Hoefner and Fogler also built the network model to simulate the wormholing process. Network model can be used to simulate different processes in porous media. While used in matrix acidizing, this model can present the evolution of wormhole structure with changes in controlling parameters. However, this method is not applicable for field design.

Hoefner and Fogler studied the three basic physical process during acidizing: acid diffusion, convection and reaction. Their work laid a foundation for setting up acid

transport equation during wormholing. However, they ignored an important factor that can affect the wormholing process significantly, fluid loss.

Hung et al.(1989) studied the effect of acid diffusion, acid convection and fluid loss. A mechanistic model was developed and sensitivity analysis was carried out. They found that wormhole length increases with increasing injection rate, decreases with increasing fluid loss rate, and decreases with increasing diffusion rate.

While investigating the wormholing mechanism, the research is also focused on the optimum condition for carbonate acidizing. Numerous lab experiments indicate that the optimum injection rate exists for carbonate acidizing. Wang (1993) conducted a series of experiments and confirmed that the optimum injection rate does exist, which leads to minimum acid used and best stimulation result. This optimum injection rate becomes the most important parameter in the following carbonate matrix acidizing models.

Huang et al (2000) developed a theory to predict the optimum injection rate, and tested it with experimental data. A cylindrical flow model is developed to represent the flow field around a wormhole propagating from a wellbore, which illustrates how to translate laboratory results to field conditions.

Linear coreflood experiments cannot reflect the flow conditions as in field, so radial coreflood experiments were done to find the wormhole structure and optimum injection rate. Frick et al (1994) conducted radial coreflood experiments and demonstrated the optimum injection rate exists in radial flow conditions. They found that this flow rate is significantly lower than the field practice. Using the same setup,

Mostofizadeh and Economides (1994) did further experiments and developed a simple method to upscale the lab results to field conditions.

McDuff et al (2010) conducted a large-scale radial-flow acidizing experiment using a 14 ft^3 cubic block. They drilled a hole in the center as the wellbore and injected acid from there. The block was scanned by high energy CT scanner. The images clearly showed the wormhole distribution and wormhole density along the wellbore. Besides, they also developed a model to simulate the pressure drop during their experiment and obtained a good agreement between the model and the experimental observation. **Fig. 1.1** shows the CT scan image of wormholes in their experiment.

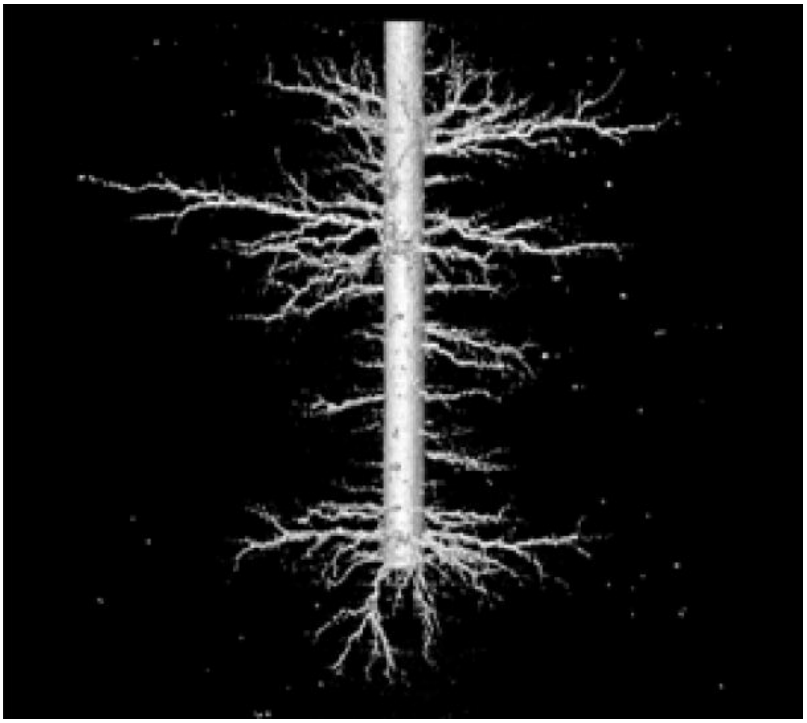

Fig. 1.1—Radial wormhole by CT scan (McDuff et al., 2010)

For field operation, if we know the wormhole density and its distribution, we can estimate the volume of acid needed. Gdanski (1999) proposed a method to estimate wormhole density. Huang et al (1999) predicted the wormhole density by modeling the pressure field around a wormhole. By combining this wormhole density model with a wormhole propagation model, the acid volume needed to penetrate a given distance can be determined.

Buijse and Glasbergen (2005) developed a semiempirical model to predict the pore volume for wormholes to break through the core and wormhole propagation rate. Their model is easy to use and only needs two parameters, optimum interstitial velocity and the corresponding pore volume to breakthrough. These two parameters can be obtained by experiments. Furui et al. (2010) calculated the tip acid velocity using finite element method and incorporated it into Buijse and Glasbergen's model, which leads to an integrated flow model. However, the basic parameters required are still the optimum interstitial velocity and the corresponding pore volume to breakthrough.

The problem comes to how to determine the two values for the wormhole models. Untill now, it is reliable to get these two parameters only from coreflood experiments. Wang et al (1993) conducted these experiments using limestone and dolomite under different temperature and acid concentration. Fredd and Fogler (1999)'s experiments were under different acid and temperature. Bazin (2001) conducted comprehensive experiments with different core lengths, acid concentration under different temperature. Talbot and Gdanski (2008) summarized their data and fitted them by Buijse and Glasbergen's model shown from **Fig. 1.2** to **Fig. 1.4**. Besides, how to

scale up the lab results to field operation is also remained a problem. Generally, it is difficult to scale up the linear acid flooding test to the field operation due to the core-size effect (Buijse, 2000). Under identical conditions, side branches are more developed in larger diameter cores. Besides, the core length will also affect the wormholing process. Bazin (2001) found the optimum injection rate increases with the increasing core length. Therefore, the first step to ensure the lab data are reliable is to eliminate the core-size effect.

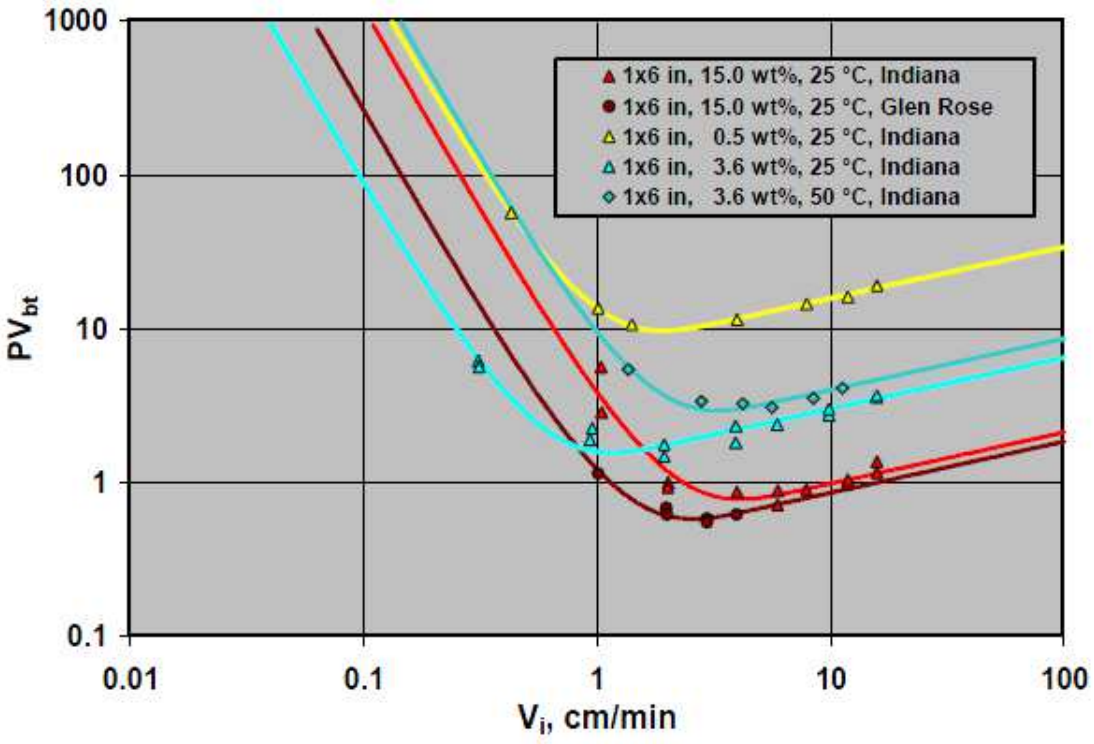

Fig. 1.2—Experiemntal data and fitting curve of Wang's data (1993)

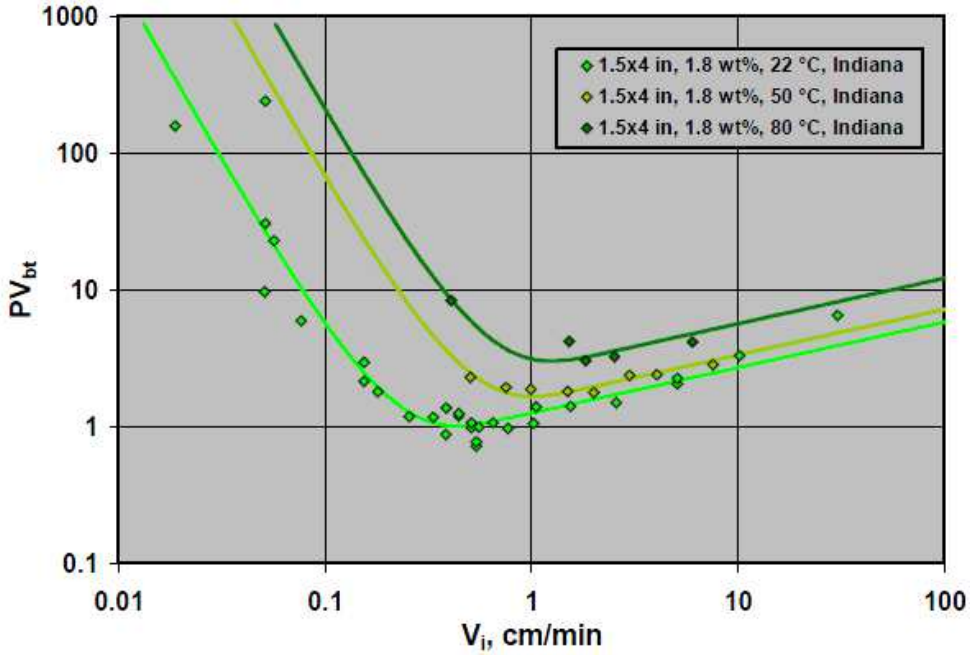

Fig. 1.3—Experiemntal data and fitting curve of Fredd and Fogler's data (1999)

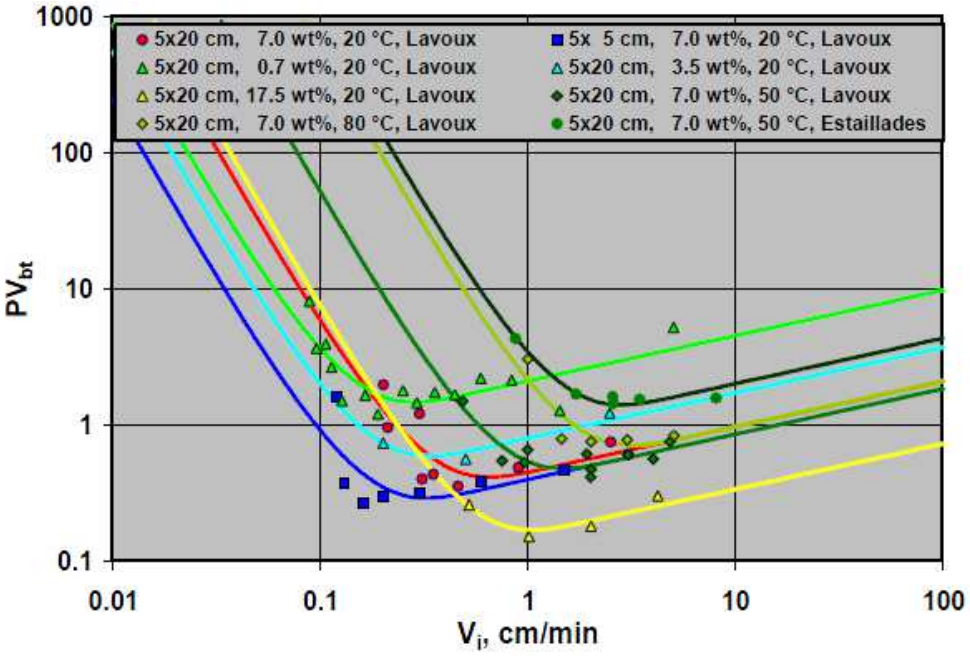

Fig. 1.4—Experiemntal data and fitting curve of Bazin's data (2001)

The research in carbonate acidizing went through from the pore scale to field scale. For pore scale research, pore enlargement and collision were investigated. For wormhole scale, transport equations coupled with reaction and diffusion were developed. For core scale, optimum injection rates are identified, and different methods for scaling up this condition to field practice are developed. Even though theoretical work has proved the existence of optimum injection rate and demonstrated the ability of models ranging from simple to extremely complicated wormhole formation, little work has been reported to predict the optimum injection rate under field conditions. There exists a need to scale up the lab results to field condition (Glasbergen et al., 2009).

1.3 Objectives of this Study

This research will investigate the influence of the core length on the $V_{i\text{-opt}}$. Once the $V_{i\text{-opt}}$ is found to remain constant when the core length reaches a certain value, it will be easier for the future research to choose the cores with appropriate length of the same rock.

Indiana limestone is used in this study. Since Indiana limestone is more homogeneous than other rocks that are available, so the results are not affected by the rock heterogeneity. Two series of experiments will be done, with one series for 1-in. diameter cores and the other series for 1.5-in. diameter cores. Each series contains four groups of experiments. The core length in one individual group is same. The lengths for 1-in. diameter cores are 1 in., 2 in., 4 in. and 6 in. The lengths in 1.5-in diameter cores are 4 in., 6 in., 8 in. and 10 in. The 1.5-in. diameter core holder can support maximum 20

in. length. Therefore, if $V_{i\text{-opt}}$ does not remain a constant from 8-in. length to 10-in. length, longer cores will be needed.

2. EXPERIMENTAL APPARATUS

2.1 General Scheme for the Setup

The setup for this research is shown in **Fig. 2.1**. The experimental apparatus includes a syringe pump, two accumulators, a core holder, a pressure transducer, a hydraulic pump, a backpressure regulator and a data acquisition system.

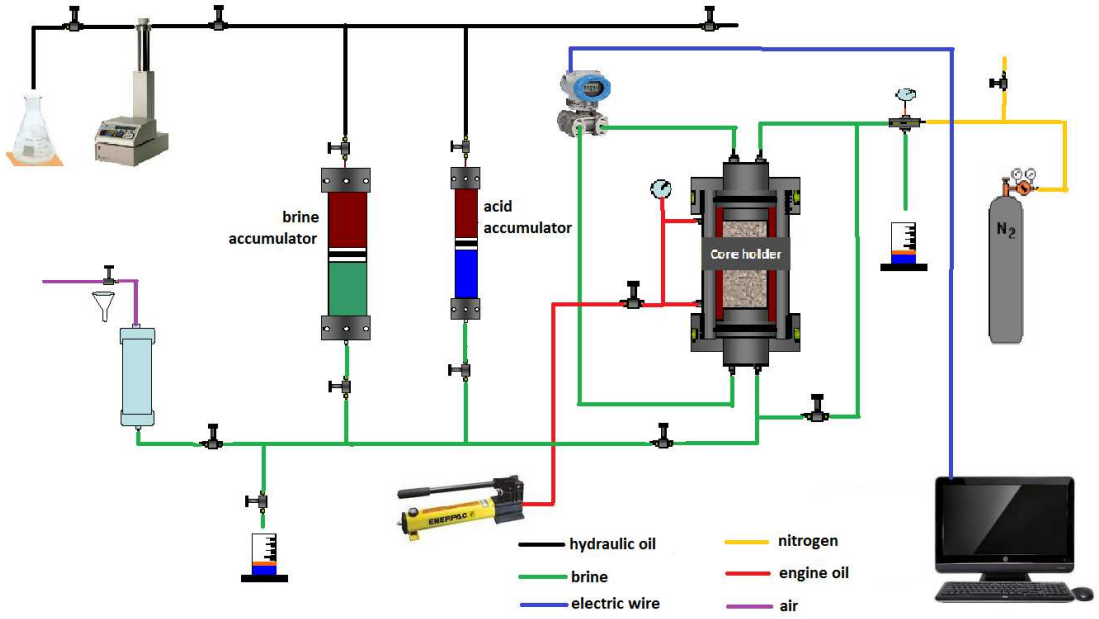

Fig. 2.1—Scheme for the setup

2.2 Syringe Pump

The syringe pump shown in **Fig. 2.2** is used to pump the fluids during experiment, either in constant flow rate mode or constant pressure mode. It can

continuously deliver flow rate over a range of 0.1 ml/minute to 400 ml/minute, at a pressures range of from atmospheric to 2,000 psi. In this research, the constant flow rate mode is used for all of the experiments. The specification for the pump is shown in **Table 2.1**.

Fig. 2.2—Syringe pump

Table 2.1—Syringe pump specification (Teledyne Isco, Inc., 2012)	
Capacity	1,015 ml
Flow range	0.100 – 408 ml/min
Flow accuracy	0.5% of set point
Displacement resolution	25.4 nl
Motor stability	±0.001% per year
Pressure range	0 – 2,000 psi
Standard pressure accuracy	0.5% Full Scale
Optional pressure accuracy	0.1% Full Scale
Wetted materials (standard)	Nitronic 50, PTFE, Hastelloy C-276
Plumbing ports	1/4'' NPT
Operating temperature	5 – 40 ºC ambient
Power required	100 Vac, 117 Vac, 234 Vac, 50/60 Hz (specify)
Dimensions (H x W x D, cm)	103 x 27 x 45
Weight	Pump: 38.5 kg; Controller: 3kg
Standard conformity	Underwriters Laboratories Inc. (UL)

Hydraulic oil is used as the displacement fluid for the syringe pump. Set the syringe pump to the REFILL mode, and it will suck in the hydraulic oil from the container to its cylinder. Once the cylinder is full, it will automatically stop.

The screen of the pump shows the working information. The flow rate, injection pressure as well as the remaining hydraulic oil volume can be read from this screen.

One thing to remember is after refilling the pump with hydraulic oil, the air may also be sucked into the pump cylinder. Therefore, the air needs to be pumped out from the refilling port before pumping hydraulic oil into the brine/acid accumulator from another port. This process is discussed in Section 3.9 in detail.

2.3 Accumulator

The accumulators are used to store brine/acid in the system. They are manufactured by Phoenix Instruments. An HCl acid accumulator and a brine accumulator are used in this research as shown in **Fig. 2.3** and **Fig. 2.4**. A Teflon piston is set inside the accumulator, which separates the accumulator into two chambers with one side filled with hydraulic oil and the other side filled with brine/acid. During the experiment, the syringe pump pushes the hydraulic oil into the oil chamber, and the oil pushes the Teflon pistons, which will then pushes the brine/acid out of the accumulator.

Fig. 2.3—Brine accumulator

Fig. 2.4—HCl accumulator

The acid accumulator is made of special alloy material, Hastelloy C-276, with capacities of 1,000 ml. The brine accumulator is made of stainless steel with capacities of 4,000 ml. Both the inlet and outlet of the two accumulators are controlled by two valves to avoid the mixing of brine and acid.

Before the experiment, the brine/acid should be filled to each accumulator first. This is accomplished through a PVC container (shown in **Fig. 2.5**) and an air compressor. The volume of PVC container is 2,000 ml, and the air compressor in the department can provide 100 psi air flow. Fill the container with brine/acid by a funnel,

then connect the container port to the air hose, thus the air can push the fluid to the accumulator. This process will be described in Section 3.6 in detail.

Fig. 2.5—PVC container

2.4 Core Holder

Core holder is a metal cylinder where the core will be placed under certain confining pressure. The core holders are manufactured by Phoenix Instruments, made of Hastelloy C276, a Nickel-Molybdenum-Chromium alloy with the addition of Tungsten. They have excellent corrosion resistance and capable to withstand a working pressure of 3,000 psi and temperatures of about 300 ºF.

A core holder includes three parts, a main body, an inlet cap and an outlet cap. **Fig. 2.6** shows the 1.5-in diameter by 20-in length core holder assembly.

Three sizes of core holders are available in the lab, 1-in. diameter by 6-in. length, 1.5-in. diameter by 20-in. length and 4-in. diameter by 20-in. length. To investigate the effect of the core length, the first two size core holders are used.

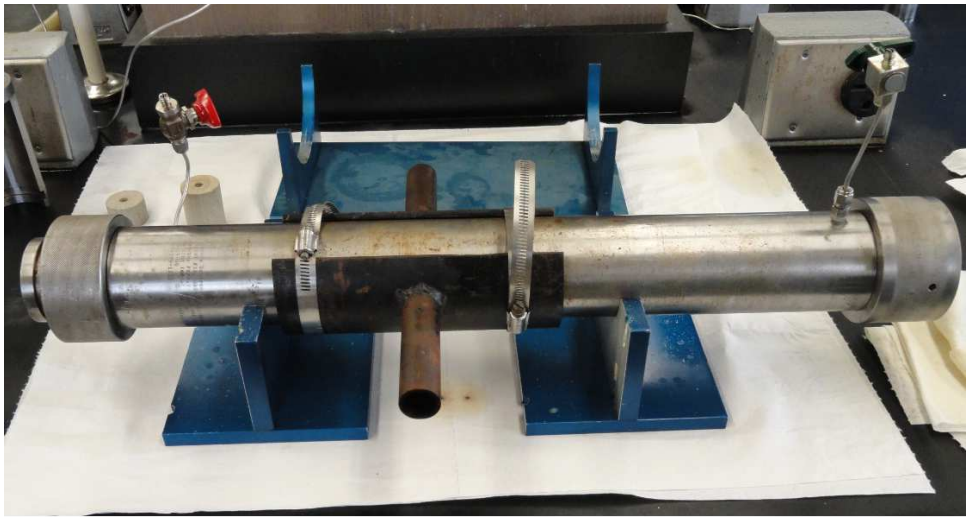

Fig. 2.6 (a)—Core holder main body

Fig. 2.6 (b)—Outlet cap

Fig. 2.6 (c)—Inlet cap

Fig. 2.7 shows the 1-in. diameter by 6-in. length core holder assembly.

Fig. 2.7—Core holder assembly with 1-in. diameter by 6-in. length

2.5 Hydraulic Pump

The hydraulic pump is used to apply the confining pressure. It is the product of Enerpac Co., Model P392. It has two stages. The first stage can supply 200 psi pressure and the second stage can supply 10,000 psi pressure at maximum. The oil reservoir capacity is 55-in.^{3}. The oil used by this pump is Shell Rotella T heavy duty engine oil. The viscosity grade is SAE 15W-40. **Fig. 2.8** shows the hydraulic pump used in the lab.

Fig. 2.8—Hydraulic pump

2.6 Backpressure Regulator

The backpressure regulator is used to regulate and control the downstream pressure of the core holder. It is set after the core holder with tubing connected to it. **Fig. 2.9** shows its structure.

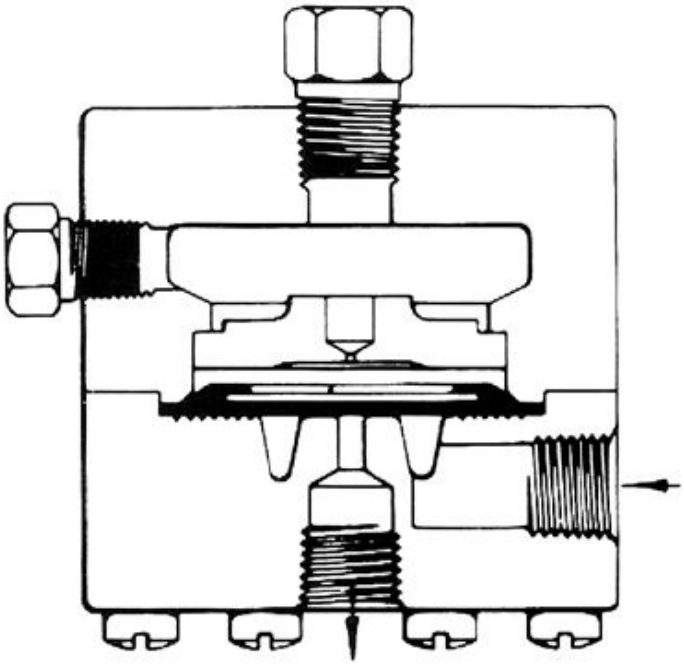

Fig. 2.9—Scheme of the backpressure regulator (Dresser, Inc., 2012)

Mity-Mite backpressure regulator, model S91-W, is used in the lab. It has two parts, the upper part and the lower part. The upper part is a dome. The dome must be charged with gas to the desired backpressure. Two connections are provided in the dome. One is intended for the attachment of a gauge and the other is connected to a nitrogen tank for dome charging purposes. The backpressure is usually set to 1,000 psi to maintain the carbon dioxide dissolved in the liquid during acid injection. The pressure behavior for the backpressure and the core holder will be explained in Section 3.8.

The lower part also has two connections, with one connection for fluid inlet and the other connection for fluid outlet. A diaphragm is set as the interface between the

upper part and lower part. The diaphragm senses the upstream pressure on the lower part and is balanced by the dome pressure on the upper part. When the pressure of the inlet fluid exceeds the dome pressure, the diaphragm will be pushed open upwards, and the fluid will enter the tiny space between the diaphragm and the lower part body, then be discharged to outside through a nozzle at the outlet connection. So the pressure of the inlet fluid is reduced. As the pressure of the inlet fluid decreases, the diaphragm moves down to reduce or shut off the flow, so that the fluid cannot go through the nozzle. In this way, the pressure of the inlet fluid will be held constant to the dome pressure dynamically.

To check if the backpressure regulator works properly or not, follow the procedure below.

- Apply a certain pressure to the regulator by nitrogen.
- Inject water to the inlet of the regulator by the syringe pump.
- Monitor the syringe pump pressure and the outlet of the regulator. If water comes out from the outlet of the regulator while the syringe pump pressure is still less than the nitrogen pressure, it means the regulator is not working appropriately. If the water comes out and at the same time, the syringe pump pressure equals the nitrogen pressure, it indicates the regulator is working accordingly.

Backpressure is necessary during the experiments at the downstream of the core to simulate the reservoir pressure. At static condition, the pressure inside the core equals

to the backpressure. When the water is injected to the core, the pressure inside the core is higher than the backpressure. **Fig. 2.10** shows the backpressure regulator used in the lab.

Fig. 2.10—Backpressure regulator

2.7 Data Acquisition System

The data acquisition system includes a pressure transducer, a NI signal processing board, and a computer installed with Labview software.

The pressure difference across the core is recorded by the pressure transducer. The transducer used is FOXBORO differential pressure gauges, models IDP10-T26 (C-D-E) 21F-M2L1.

A diaphragm is set inside the pressure transducer to sense the pressure difference of its two sides. This diaphragm will bend under pressure difference, and this bending will be translated to an electrical signal which will be received by the processing board.

In the acidizing experiment, the inlet port is connected with the inlet of the core holder by the tubing and the outlet port is connected with the outlet of the core holder. In this way, one side of the diaphragm senses the inlet pressure of the core while the other side senses the outlet pressure of the core. The pressure transducer thus will show the pressure difference across the entire core at each time step. **Fig. 2.11** shows the pressure transducer used in the lab.

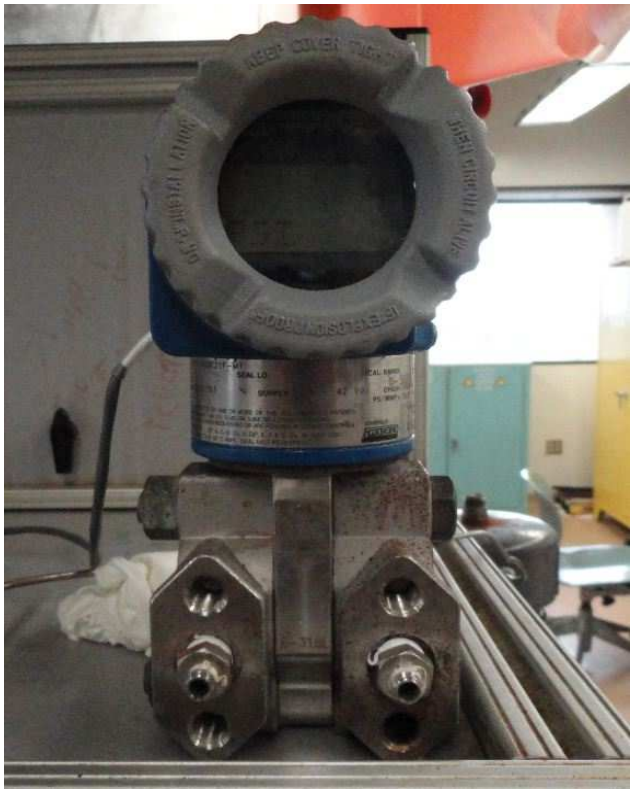

Fig. 2.11—Pressure transducer

The pressure transducer will output an electric signal to a signal processing board shown in **Fig. 2.12**. The NI CB-68LP board is used to receive the electric signal from the transducers, and transfers the signals to the main board inside the computer.

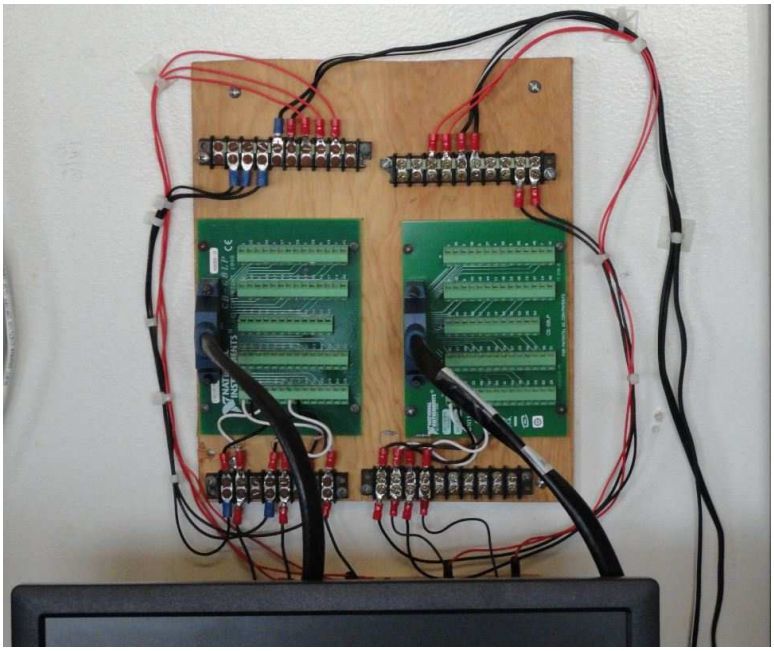

Fig. 2.12—Signal processing board

A program is written to read and process the signals from the main board. This program is encapsulated into a VI file. The Labview software is used to open and run this VI file. It records the data every five seconds and writes it into a data file dynamically. Before starting to run the VI file in the Labview, the directory of the data files needs to be specified. Microsoft Excel is used to open this data file and generate graphics based on these data recorded. The methods for operating this software are illustrated in detail in Appendix.

3. EXPERIMENTAL PROCEDURE

This section describes the experimental procedure in detail, including preparation part and injection part. In order to start the injection, cores and acid should be prepared beforehand. The core needs to be saturated so that porosity and pore volume can be obtained. Once the preparation is completed, the injection can be started. Section 3.1 gives a general scheme for this experiment. Section 3.2 to 3.6 describes the pre-experimental preparation procedures in detail. Section 3.7 describes the procedures for injection. Section 3.8 analyzes pressure behavior during experiment and Section 3.9 discusses method to get rid of the air inside the system.

3.1 General Description for the Experiment

Before describing the experimental operation in detail, the general procedure for acidizing experiment is present as below.

1. Dry the cores in the oven and measure the dry weight.
2. Saturate the cores with brine in the vacuum pump for 24 hours, and measure the wet weight. Calculate porosity.
3. Prepare 15 wt% HCl and then fill the acid accumulator with the acid.
4. Fill brine to the brine accumulator.
5. Put the core in the core holder and fix it on the setup shelf.
6. Set the syringe pump with desired flow rate. Apply 1,000 psi backpressure.

7. Run the syringe pump to fill the tubing with brine, until the whole system is pressurized (core outlet pressure equals the backpressure applied by the nitrogen).
8. Inject brine till the pressure drop is stabilized, so that the permeability can be calculated by Darcy's law.
9. Open the acid valve and close the water valve swiftly to begin the acid injection. Start the timer.
10. Stop the timer when the pressure difference declines sharply to around 15 psi (When the wormhole breaks through the core, the pressure difference is 15 psi in this lab. It is just experience.). Record the time.
11. Open the brine valve and close the acid valve.
12. Release the backpressure and flush the system with brine.

3.2 Core Cutting

The lithology of the cores used in this research is Indiana limestone, with permeability around 7 md and porosity of 15%. Indiana limestone is more homogeneous than other carbonates, so the properties are more consistent along the cores. The cores are provided by Kocurek Industry Co.

The core dimensions for this research are listed in **Table 3.1**.

Table 3.1 Core dimensions

Diameter, in.	Length, in.			
1	1	2	4	6
1.5	4	6	8	10

The 1-in. diameter core holder can only support 6-in. length at maximum. Realized that this length may not be long enough to study the core length effect, therefore, the 1.5-in. diameter cores are also used in this study since the 1.5-in. diameter core holder can support a maximum length of 20-in.

3.3 Core Treatment

Before the experiment, the core samples are numbered, and then dried in the oven for two hours so that the vapor in the pore space can escape completely. After taking the cores out of the oven, measure the weight of each core, which gives the dry weight.

The next step is to saturate the core. This is accomplished through a vacuum pump (**Fig. 3.1a**). The vacuum pump can be connected to two types of containers, the PVC container (**Fig. 3.1b**) and the glass bell container (**Fig. 3.1c**).

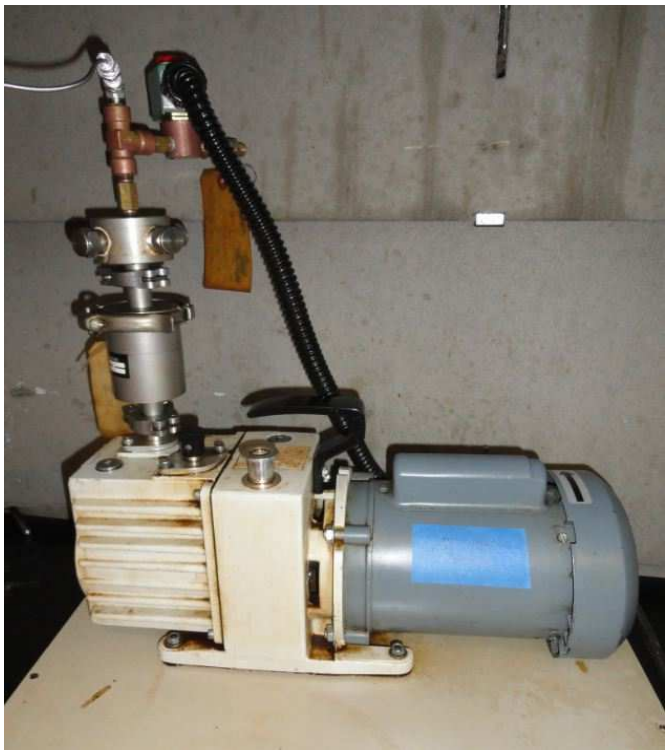

Fig. 3.1 (a)—Vacuum pump

Fig. 3.1 (b)—PVC container

Fig. 3.1 (c)—Vacuum glass bell

The details for saturating cores are given below.

- Make sure the container is clean. Put sufficient amount of brine so that the core samples are submerged completely.
- Apply some grease on the container's lid rim, so that the container can be sealed firmly.
- Connect the container to the vacuum pump by a hose or metal tubing.
- Start the vacuum pump and keep it running for 12 hours.
- After running 12 hours, stop the pump for one hour to cool down the pump.
- Start the pump again and run another 12 hours.
- Stop the pump and take the cores out from the vessel, merge them in another container with same type of brine. Try to use these cores as soon as possible, for the minimum changes of the core properties.

3.4 Porosity Measurement

Once the cores are fully saturated, measure the weight of these saturated cores, and the porosity can be calculated. Porosity is the ratio of pore volume over core bulk volume. The porosity is calculated by

$$V_{\text{bulk}} = A \cdot L = \frac{1}{4}\pi d^2 \cdot L \tag{3.1}$$

$$V_{\text{pore}} = \frac{M_{\text{saturated}} - M_{\text{dry}}}{\rho_{\text{brine}}} \tag{3.2}$$

$$\phi = \frac{V_{\text{pore}}}{V_{\text{bulk}}} \times 100\% \tag{3.3}$$

3.5 Acid Preparation

The acid used in this research is 15wt% HCl. The raw commercial acid used in the lab is produced by MACRON Chemical Co. with weight percent of 36.5%. It can be purchased from the Bio & Bio Chemistry Shop on the campus of Texas A&M University.

In order to prepare 15wt% HCl, certain proportion of water and raw acid need to be mixed. **Table 3.2** shows the proportion of water and raw acid for the experiment acid.

Table 3.2 Proportion for water and raw acid

Hydrochloric Acid	Concentration, weight percent	Density, g/cm^3	Volume, ml
Raw acid	36.5	1.185	95
Water	0	1.0	155
Experiment acid	15	1.07	250

Weight percent is how much mass of HCl in a unit mass of the solution. The desired acid concentration for experiment can be calculated as shown below.

$$C_{\text{experiment\_acid}} = \frac{V_{\text{raw\_acid}} \cdot \rho_{\text{raw\_acid}} \cdot C_{\text{raw\_acid}}}{V_{\text{raw\_acid}} \cdot \rho_{\text{raw\_acid}} + V_{\text{water}} \cdot \rho_{\text{water}}} \tag{3.4}$$

3.6 Refilling Brine and Acid

The brine and acid should be filled to the accumulator before the injection. We have stated that this is accomplished by the PVC container and an air compressor. **Fig. 3.2** shows the tubing connections for this operation.

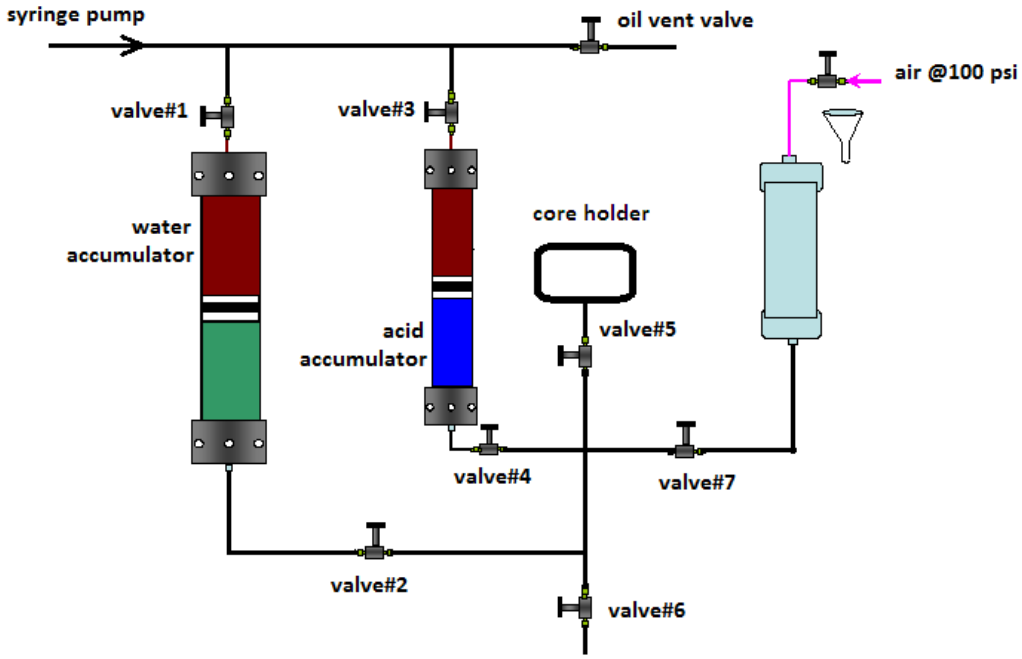

Fig. 3.2—Scheme of the refilling part

There are two acid accumulators in the lab. They are intended to contain HCl and HF respectively. In this research, only HCl accumulator is used. Valve #5 in Fig. 3.2 is connected to the core holder, while valve #6 is for discharging liquid. Valve #5 is closed all the way during this operation. The air supply comes from the central air compressor

in the department. The air pressure is 100 psi, and the air flow rate can be controlled by the supply valve mounted in the lab.

The steps for the refilling are described below.

1. Make sure there is no acid in acid accumulator. Close valve #1 and #2 and open valve #3 and #4. Start the Syringe pump to push the hydraulic oil to the acid accumulator, until no liquid comes out from valve #6, which means the piston inside the acid accumulator has reached the bottom. Then close valve #3 and #4 of the acid accumulator. Note that during this operation, both valve #5 and valve #7 are closed.
2. Flush the tubing with water. Fill some water to the PVC container; connect it with the air supply. Open valve #1, valve #2 and valve #7. Open the air supply valve and fill some water to the brine accumulator. Pay attention to the oil vent valve to see if the hydraulic oil comes out or not. If not, close the air supply valve immediately and check the problem. After some water has entered the brine accumulator, stop the air and discharge the remaining water in the PVC container. Close the oil vent valve and run the syringe pump to push the water out from the brine accumulator, so that all the tubing between the accumulator and the core holder are flushed.
3. Begin refilling brine to the brine accumulator. First fully fill the brine to the PVC container and connect it to the air supply. Check the status of all the valves. Make sure valve #1, valve #2, valve #7 and the oil vent valve

are open and the rest of the valves are closed. Open the air supply valve, so that the air will push the brine to the brine accumulator, and the hydraulic oil will be vented to a vessel. The brine volume that has been refilled equals the volume of hydraulic oil that has been vented. The vessel with the volume mark is recommended. It is suggested that half volume of PVC container being refilled each time, so that the air may not enter the accumulator with liquid. If more liquid is needed, fully refill the PVC container again, and begin the air supply. Control the air supply valve to avoid too high air flow rate.

4. Begin refilling acid to the acid accumulator. Follow the same procedure as refilling brine. Remember to make sure the valves are in the right status. When the refilling is finished, run the syringe pump to push some of the acid out from the acid accumulator. This is to pump out the air in the acid accumulator, since there is possibility that the air might enter the acid accumulator together with acid during refilling. After that, close the valve #3 and valve #4.
5. After refilling the acid, the tubing needs to be flushed to remove the acid inside. Run the syringe pump to pump the brine out from the brine accumulator for a while. Use the PH tester to test the fluid coming out from valve #6. If it is neutral, stop the pump. The refilling is finished.

3.7 Procedure for the Injection

Put the core in the core holder. Attach the inlet cap and the outlet cap. If the core is not long enough, add a spacer inside the core holder. Mount the core holder on the shelf. After that, the first thing is to apply confining pressure to the core holder. Simply connect the hydraulic pump to the lower port of the core holder. When the hydraulic oil goes into the annular space between the sleeve and the core holder body, it can push the air inside out from the upper port of the core holder. So when the oil comes out from the upper port, it indicates the air has been pushed out. Close the valve of the upper port so that the confining pressure can be built up. Usually, apply 300-400 psi for the confining pressure at this time.

After applying the confining pressure, connect the tubing to the right port. **Fig.3.3** shows the tubing connection for this part.

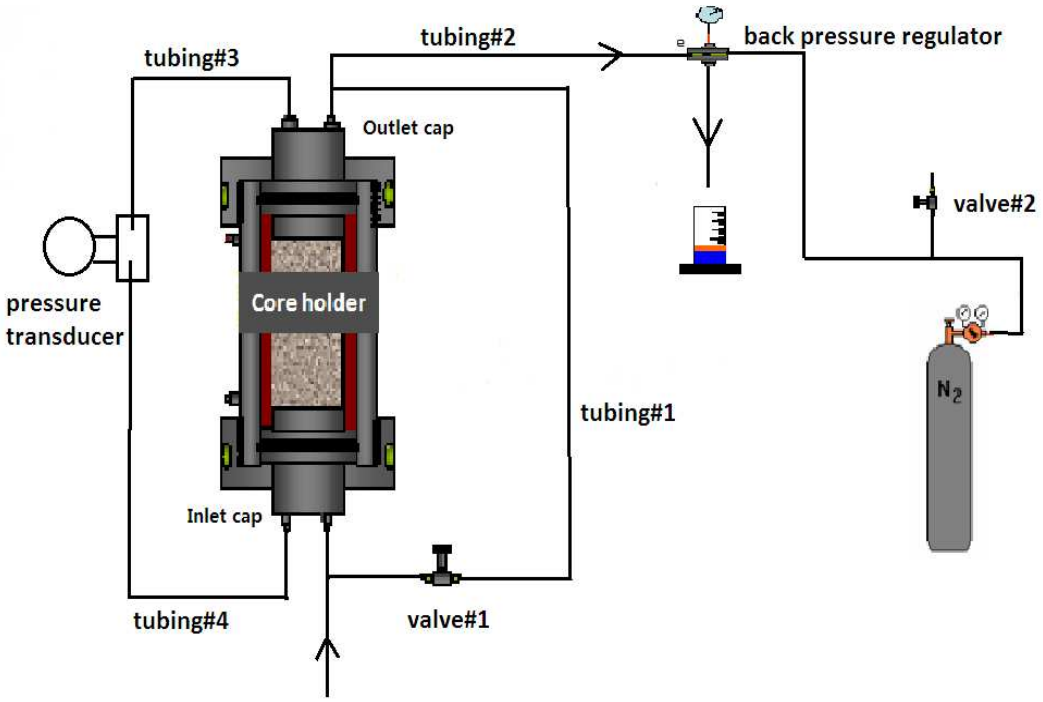

Fig. 3.3—Tubing connection for the core holder

The inlet cap of the core holder has two ports. One port is connected to the inlet of the transducer and the other port is connected to the outlet of the brine/acid accumulator. The outlet cap of the core holder also has two ports, with one port connected to the outlet of the transducer while the other port connected to the backpressure regulator. In this way, the transducer will measure the pressure difference between the two sides of the core. During experiments, the pressure at the top side of the core will remain constant. It is exactly the same as the backpressure applied by the nitrogen.

Tubing #1 shown in Fig. 3.3 is necessary for this experiment. It bypasses the core holder and is directly connected to the backpressure regulator. It is used to fill all the

tubing with brine before the brine is injected to the core. The details of how it works are as follows.

1. After all the tubing is connected, start the syringe pump to pump the brine to the core holder. Meanwhile, make sure the valve #1 shown in Fig 3.3 is open. In this way, the brine will go through the tubing #1 instead of the core.
2. Continuously run the syringe pump until the brine comes out from the outlet of the backpressure regulator. Leave it running for a while and the brine will fill up all the tubing including tubing #1, tubing #2, tubing #3 and tubing #4 under the atmospheric condition.
3. The next thing is to apply the backpressure by the nitrogen tank. The backpressure in this research is set to 1,000 psi. After the backpressure is applied, the brine stops coming out from the outlet of the backpressure regulator since the upstream pressure is lower than the backpressure.
4. Keep the syringe pump running until brine comes out from the outlet of the backpressure regulator again. During this period, the syringe pump is building up pressure to push the brine out. The backpressure acts as an obstacle which stops the route of the brine. Therefore, when the pressure of the fluid is high enough to move this obstacle, the fluid will go out. After a while when the pump has built up a sufficient pressure that is higher than the backpressure, the fluid will flow out. Notice that if the fluid flows out when the syringe pump pressure is lower than the

backpressure, it means that the backpressure regulator is out of work. During this period, monitor the syringe pump pressure and adjust the confining pressure. Make sure the confining pressure is always at least 400 psi higher than the pump pressure. The duration for this period depends on the injection rate. Usually 20 ml/min is preferred so that the pressure will not build up either too fast or too slow.

5. To this point, the whole system is pressurized and the core outlet pressure equals to the backpressure. The core is simulated in a reservoir condition with 1,000 psi reservoir pressure.

When the pressure in the system has reached the backpressure applied by the nitrogen, it is a good time to check if there are leaks in the system because some leaks only appear under high pressure.

The next step is to set the flow rate as desired flow rate and keep it running for about one minute so that the flow in the tubing will be stable. Meanwhile, get ready for the Labview software. Then close valve #1 so that the brine will flow through the core. Start the Labview program. The principle for choosing injection rate will be discussed in Section 4.2 and the procedure for running Labview is described in Appendix.

During experiment, the following items should always be checked to make sure the experiment is in the correct progress.

- Check the liquid flow rate from the outlet of the backpressure regulator. This is a closed system and the mass is conserved. Due to the incompressibility of the brine and the hydraulic oil, the amount of the

brine that is pumped into the core should equal the amount of the brine coming out. Therefore, if there is no liquid coming out, or the amount of liquid coming out is significantly less than the amount that is pumped in, the experiment should be stopped. It is probably because either there is air trapped in the system or there are leaks somewhere in the system.

- Check the syringe pump pressure and adjust the confining pressure. Make sure the confining pressure is at least 400 psi higher than the core inlet pressure, which is also the syringe pump pressure. 400 psi comes from experience. Usually if the difference between the confining pressure and the core inlet pressure is more than 400 psi, the brine cannot go along the annular space between the sleeve and the core.
- Check all the joints to see if there are leaks. If any leak is found, stop the experiment, fix the leak and restart.

For a typical coreflood experiment, the pressure difference buildup curve is shown in **Fig. 3.4**. The pressure difference equals to the core inlet pressure minus the core outlet pressure, which is also referred as the pressure drop across the core. It can build up to 90% of the total pressure drop within the first 10 minutes. When the pressure difference is stable, the flow has reached steady state and the permeability can be calculated based on the Darcy's law, and the system is ready for acid injection. The procedure for switching to acid and time recording is described below.

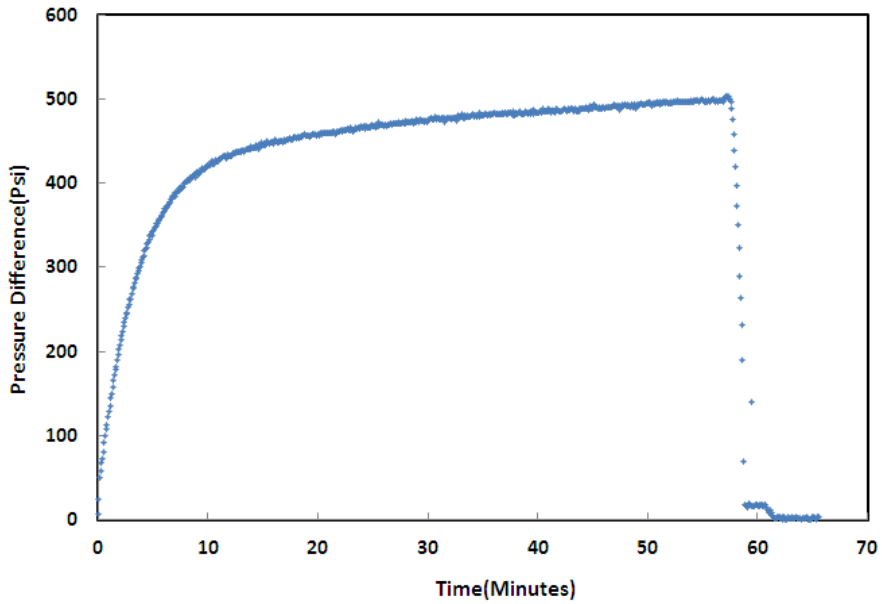

Fig. 3.4—Typical pressure difference curve for acidizing experiment

Switching from brine to acid relies on the four valves shown in **Fig. 3.5**. The valve #2 and #3 are open while valve #1 and #4 are closed during brine injection. Follow the sequence below to switch the valves.

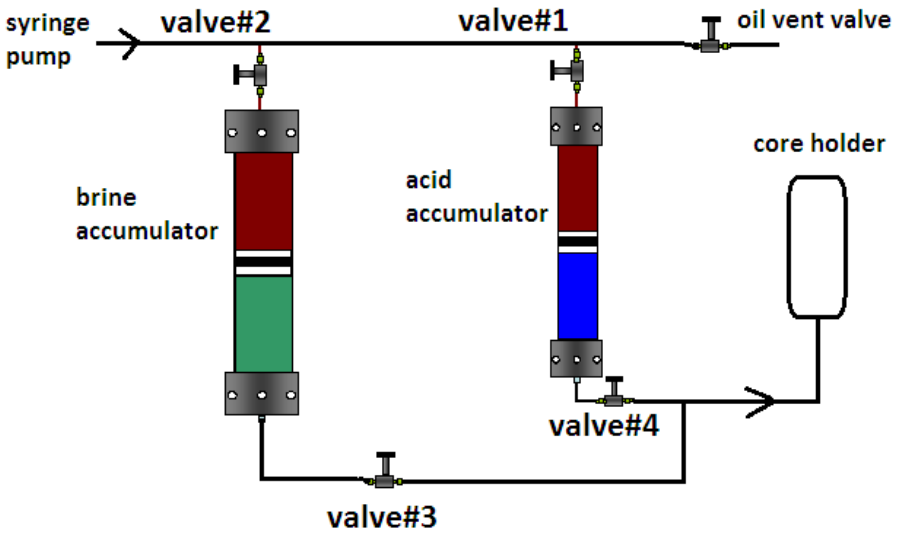

Fig. 3.5—Scheme for switching valves

1. Open valve #4
2. Open valve #1, begin recording time
3. Close valve #2
4. Close valve #3

These should be done as quickly as possible so that the brine and the acid will not mix.

There is a sharp pressure drop in Fig. 3.4 at the time of around 60 minutes, when the acid is being injected. This is because of the growing wormholes. With further penetration of the wormhole, the equivalent core length decreases, so the pressure drop across the core decreases. Finally when the wormholes break through the core, the pressure drop for fluid flow along the core is negligible.

Once the wormhole breakthrough is observed from the dynamic pressure difference curve, stop the timer and write down the time for acid injection. The brine should then be switched back from the acid, following sequences below.

1. Open valve #2
2. Open valve #3
3. Close valve #1
4. Close valve #4

The final step for the experiment is to release the backpressure. This step should be done slowly with caution since the system is at high pressure condition. Besides, the confining pressure and core inlet pressure should also be considered. Keep the confining pressure within 200 psi higher than the inlet pressure to avoid the core break. **Fig. 3.6** shows a part of the setup which will be used when release the backpressure. The sequence for this job is described below.

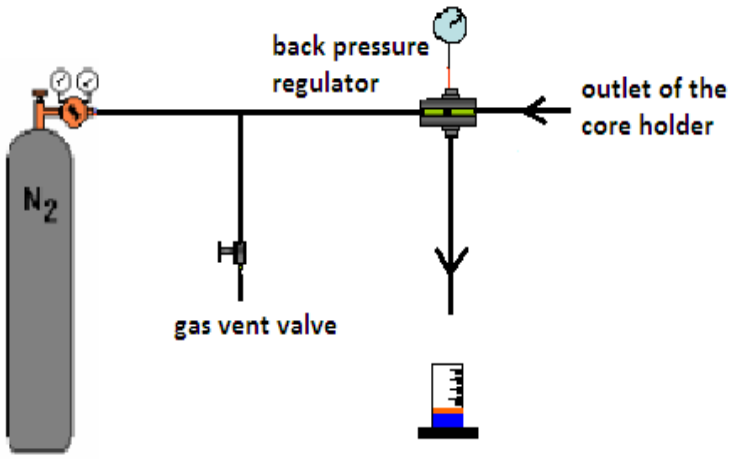

Fig. 3.6—Scheme for releasing backpressure

1. Open the gas vent valve to 20° (90° is the full range), some nitrogen will come out.
2. Turn off the nitrogen tank regulator a quarter of its full range (the full range is 9 rounds), the backpressure will also go down.
3. Release the confining pressure. Make sure it is within 200 psi higher than the core inlet pressure. 200 psi can assure that the confining pressure is either not too high to break the core or too low to hold the fluid inside the core holder. Note that at this time, the core inlet pressure almost equals to the backpressure, so the backpressure gauge can be used for convenience.
4. Continue to release the backpressure till zero, and meanwhile release the confining pressure. Still, make sure that the confining pressure is within the range of 200 psi higher than the core inlet pressure so that the core will not break.

After the backpressure is released, the experiment is completely finished. The next step is to take the core holder apart and take the core out. Wash the core and core holder using water and then keep them.

There is still acid left in the acid accumulator. If another experiment is needed after the previous one, the acid can be used. Otherwise, pump all the acid out, refill water to the acid accumulator and pump the water out, thus to flush the acid accumulator.

After pumping out the acid, flush the system using water.

3.8 Pressure Analysis

Pressure behavior is an important indicator for the experiment. It can be used to judge whether the experiment is valid or not. The relationship between syringe pump pressure, core inlet pressure, core outlet pressure, backpressure and confining pressure should be clearly understood.

- The backpressure applied by the nitrogen tank on the backpressure regulator is fixed. It will not change during the experiment.
- The pressure at the core outlet equals to the backpressure. It will not change either.
- The pressure transducer always shows the pressure difference across the core. At the beginning of the experiment during the transient flow period, the pressure difference increases fast, while when the flow reaches steady state, the pressure difference fluctuates around a constant value.
- The pressure at the inlet of the core equals to the backpressure plus the pressure difference. Therefore, it increases fast during the transient flow period and fluctuates around a constant value when the flow reaches stable condition.
- The pressure of the syringe pump equals to the core inlet pressure.
- The confining pressure applied by the hydraulic pump should be adjusted all the time since it is directly related with the core inlet pressure. Always make sure that the confining pressure is at least 400 psi higher than the core inlet pressure during the fluid injection.

3.9 Air Analysis

This setup is a closed system filled with incompressible fluids. Therefore, the volume of brine coming out should equal to the volume of hydraulic oil pumped in. However, if air is trapped inside the system, the fluid becomes compressible. The volume of brine coming out cannot be predicted. So the air should be eliminated from the system before an experiment.

In order to get rid of the air, the air sources should be identified. There are three ways that the air can enter the system, from the syringe pump, from the PVC container and from the tubing.

When the syringe pump refills the hydraulic oil from the container, the air may also be sucked in, and accumulates inside the pump cylinder. When the pump is started, the air can be pumped to the brine/acid accumulator together with the hydraulic oil. Therefore, it is necessary to push the air out from the pump cylinder before starting the experiment. **Fig. 3.7** shows the scheme for this part.

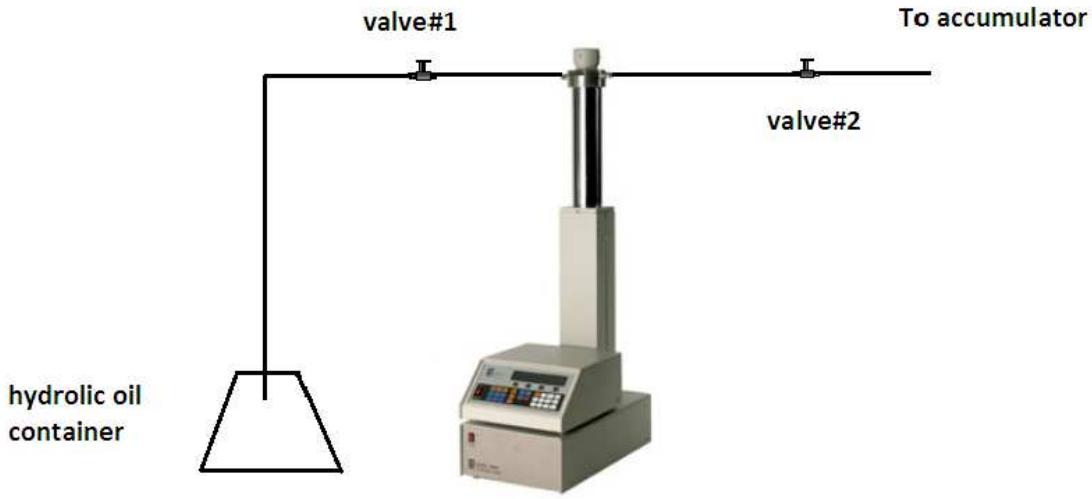

Fig. 3.7—Scheme for pumping air out of the syringe pump

The method for pumping out the air is described below.

- Open valve #1 and close valve #2, set the syringe pump to the REFILL mode and fully refill the pump cylinder.
- Stop the pump. Leave the pump still for several minutes so that the air can accumulate inside the top part of the pump cylinder.
- Keep valve #1 open and valve #2 closed. Run the pump to pump out the hydraulic oil and air. Air bubbles can be seen in the hydraulic oil container.
- Keep the pump running until no bubbles can be seen inside the container.
- Stop the pump, close valve #1 and open valve #2.

When the air is pumped out from the pump cylinder, this pump is ready for use.

The air can also go into the system during brine/acid refilling from the PVC container. It is suggested (Section 3.6) that half volume of PVC container being refilled each time, so that the air may not enter the accumulator with liquid. And control the air supply valve to avoid large air flow rate.

Before an experiment, the tubing is filled with air. So it is necessary to fill them with brine before the connection.

It has been stated that the pressure drop within the first 10 minutes can build up to 90% of the total pressure drop when the flow is stabilized. If it takes much longer time for the pressure drop to build up, there is possibility that the air is inside the system.

4. RESULTS & DISCUSSION

This research aims to study the effect of the core length on the optimum acid injection rate. Two series of experiments are conducted to achieve this goal. The cores used have two diameters, either 1 in. or 1.5 in., but the length varies. This section will introduce how to get the optimum acid injection rate from the experimental data, and the experiment results are also discussed.

4.1 Method to Get the Optimum Acid Injection Rate

The objective of this research is to find the optimum acid interstitial velocity for each group of cores, and then find the trend of these optimum acid interstitial velocities related to the core length. It is necessary to explain the basic concepts beforehand.

The interstitial velocity is the ratio of injection rate over the area open to flow. It is an average fluid velocity flowing through the porous media. It can be written as below.

$$V_i = \frac{q}{A \cdot \phi} \tag{4.1}$$

The pore volume for breakthrough is a dimensionless number that measures the amount of the acid used to break through the core in terms of pore volume. It is the ratio of the volume of the injected acid when the wormholes break through the core over the pore volume of the core. It can be written as below.

$$PV_{\text{bt}} = \frac{V_{\text{acid}}}{V_{\text{pore}}} = \frac{q \cdot t}{V_{\text{core}} \cdot \phi} \tag{4.2}$$

The pore volume for wormholes breakthrough is calculated based on the injection rate and injection time. The injection rate is set constant by the syringe pump during an experiment. The injection time is the time for acid injection minus the time for acid flow from the acid accumulator to the core inlet. It is calculated by the steps below.

1. When the acid flows out of the acid accumulator, record the local time as t_0.
2. The volume of the tubing between the outlet of the accumulator and the inlet of the core is calculated by the tubing length multiply the tubing void cross-sectional area. Since the tubing is bended, the length can be measured by a tape. The tubing diameter and wall thickness can be looked up from the product information published by the tubing company, so that the void cross-sectional area can be calculated. The time for acid flowing out from the acid accumulator to the core surface is simply calculated by the void volume over the injection rate. This duration time is marked as t_1.
3. When the wormholes break through the core, record the time as t_2.
4. When the brine valve is switched open, record the time as t_3.

So the time for wormholing process is

$$t = t_2 - t_0 - t_1 \tag{4.3}$$

With the time t, the pore volume breakthrough is calculated by equation 4.2.

When the acid attacks the core, the wormhole begins to form and the pressure difference monitored by the transducer begins to decrease due to the wormhole propagation. **Fig. 4.1** shows a typical record during an experiment.

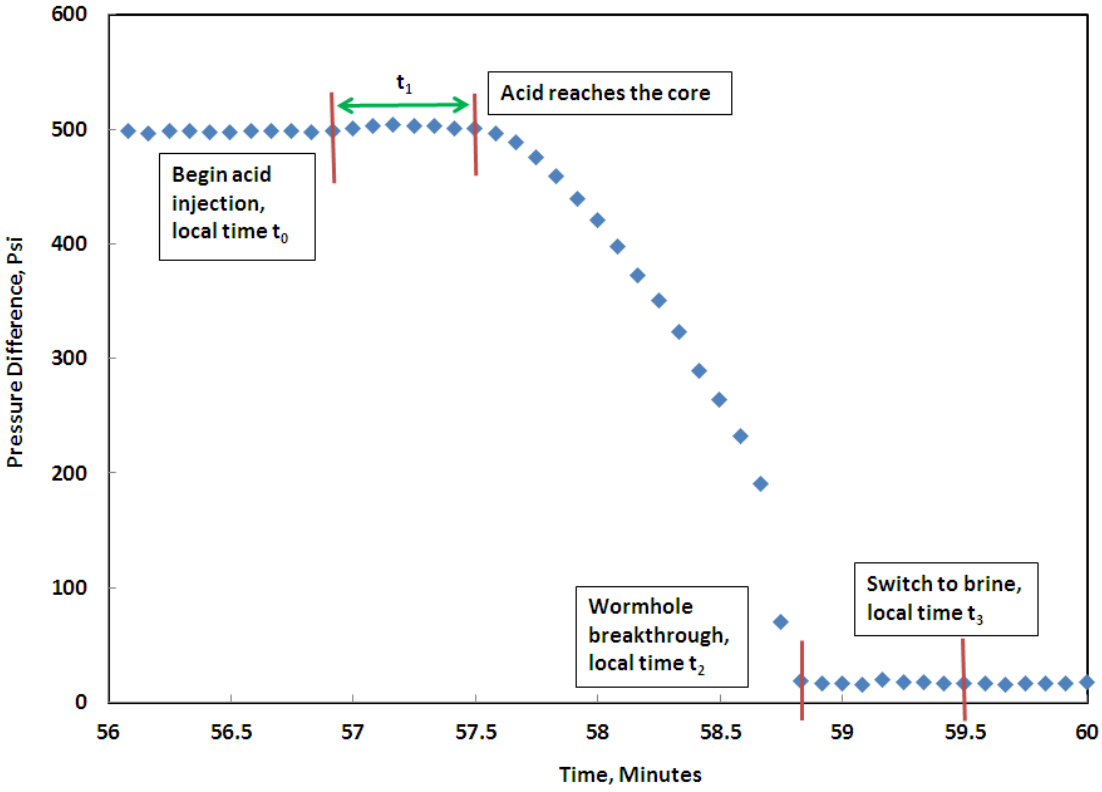

Fig. 4.1—Pressure difference curve during acid injection

The next step is to mark the points for the beginning of acid injection, acid reaching the core, wormhole breakthrough and beginning of brine injection, as shown in Fig. 4.1. The point for wormhole breakthrough can be easily identified because this is the point when the pressure difference drops to the lowest value. The VI file records the

pressure drop every five seconds. The local time for beginning acid injection and wormhole breakthrough are known. Therefore, the exact point shown in Fig 4.1 for t_0 can be determined by counting the time t_2-t_0 point by point backwards from the wormhole breakthrough point. Based on point t_0, the point for acid reaching the core can be determined by counting the duration time t_1 forwards. Based on point t_2, the point for switching brine can be determined by counting the time t_3-t_2.

For each acidizing experiment, the result that is of interest is the pore volume for wormhole breakthrough (PV_{bt}) under a certain acid interstitial velocity (V_i). For a group of cores, V_i is the only different parameter for every experiment in this group. One V_i leads to one PV_{bt}. For multiple experiments, multiple pairs of V_i and PV_{bt} can be obtained. If we take 1.5-in. diameter by 8-in. length cores as an example, 11 individual experiments were conducted for this group of cores, so correspondingly we get 11 pairs of V_i and PV_{bt} shown in **Fig. 4.2**.

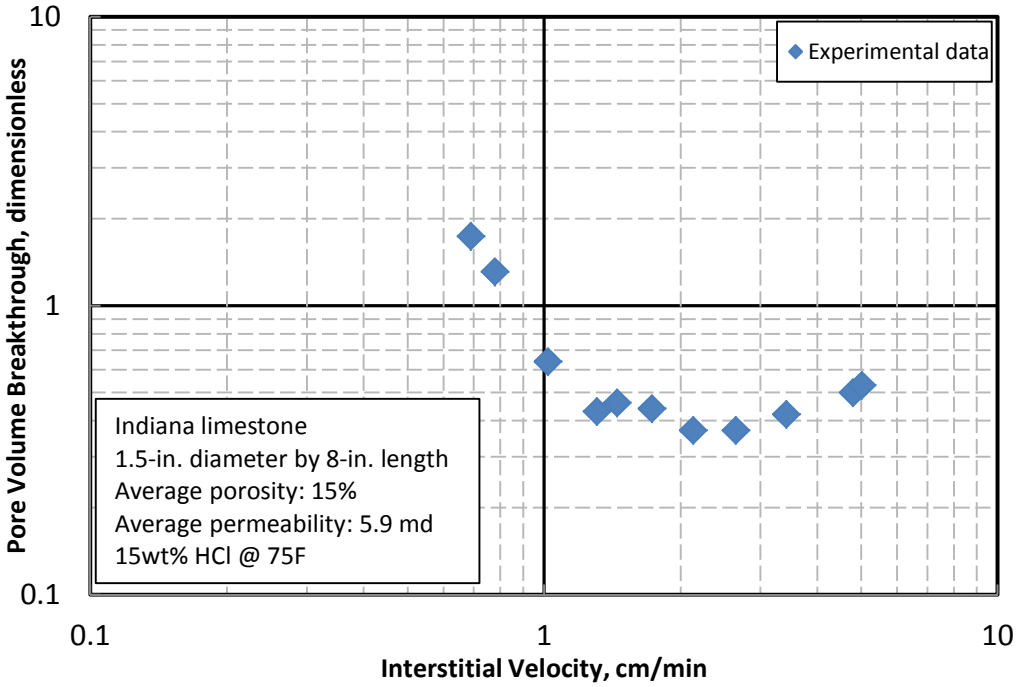

Fig. 4.2—Experimental data for 1.5-in. diameter by 8-in. length cores

Fig 4.2 presents the data points of a group experiments with 1.5-in. diameter by 8-in. length cores. A trend can be easily identified that the PV_{bt} decreases first and then increases with increasing V_i. However, the $V_{i\text{-opt}}$ is not easy to locate on this figure directly. It may not be the lowest point with smallest PV_{bt} shown in the figure. To find this optimum value, proper equations should be used to fit these data. After the fitting curve is determined, the transition point of this curve will be the optimum point.

As we have stated in Section 1.2 that Buijse and Glasbergen (2005) developed a semiempirical model to predict the pore volume breakthrough and wormhole propagation rate. Their model is used here for the curve fitting.

Buijse and Glasbergen's semiempirical model can be described below.

$$PV_{\text{bt}} = \frac{V_i^{1/3}}{W_{\text{eff}} \cdot B(V_i)} \tag{4.4}$$

$$W_{\text{eff}} = \frac{V_{i-\text{opt}}^{1/3}}{PV_{\text{bt}-\text{opt}}} \tag{4.5}$$

$$B(V_i) = [1 - \exp(-W_B \cdot V_i^2)]^2 \tag{4.6}$$

$$W_B = \frac{4}{V_{i-\text{opt}}^2} \tag{4.7}$$

The four equations present a relationship between pore volume breakthrough and interstitial velocity. They can be written as a single equation by substitution as below.

$$PV_{\text{bt}} = PV_{\text{bt}-\text{opt}} \left(\frac{V_i}{V_{i-\text{opt}}}\right)^{1/3} \{1 - \exp[-4(\frac{V_i}{V_{i-\text{opt}}})^2]\}^{-2} = f(V_i) \tag{4.8}$$

PV_{bt} and V_i can be obtained from the experiment directly. By using least squares method, the experimental data can be fitted, which will also results in $PV_{\text{bt-opt}}$ and $V_{i\text{-opt}}$.

$$J = \sum_i^n [PV_{bt}^i - f(V_i^i)]^2 \tag{4.9}$$

Where n is the amounts of experiment data. In order to get the best results, the residue J should be minimized. This can be done by selecting proper $PV_{\text{bt-opt}}$ and $V_{i\text{-opt}}$.

After $PV_{\text{bt-opt}}$ and $V_{i\text{-opt}}$ are determined, the curve can be plotted easily in Microsoft Excel. **Fig. 4.3** shows the fitting curve for a group experiments with 1.5-in. diameter by 8-in. length cores.

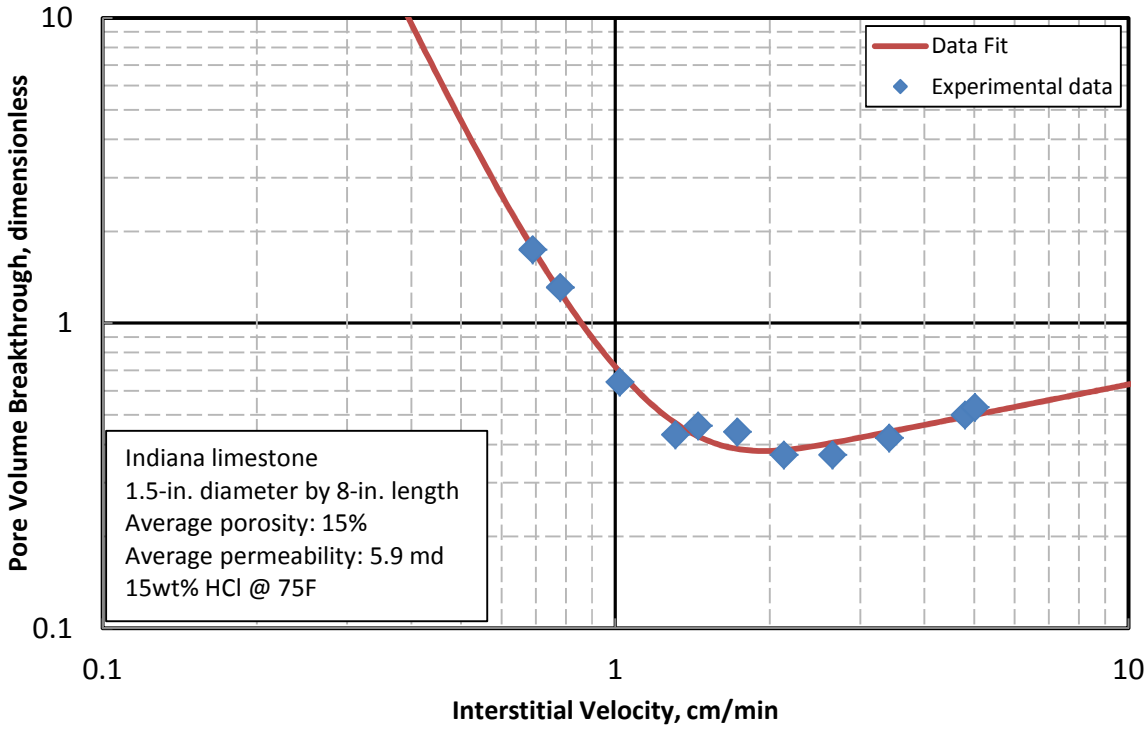

Fig. 4.3—Experimental data and curve fitting for 1.5-in. diameter by 8-in. length cores

Sometimes bad data points may exist because of experimental error. In such a case, these data will affect the curve fitting results and values for $PV_{\text{bt-opt}}$ and $V_{i\text{-opt}}$. Therefore, it is suggested eliminating the bad data points that are obviously off the trend. More experiments may be required to update the curve. Below is an example for this case.

The experimental data for the group of 1.5-in. diameter by 6-in. length cores shown in **Fig. 4.4** seem scattered. By fitting these data, the curve shown in **Fig. 4.5** can be obtained, so do the corresponding $V_{i\text{-opt}}$ and $PV_{\text{bt-opt}}$. Four yellow circular-shaped points in Fig. 4.5 are marked out. Compared with other data, they are deviated

significantly from the fitting curve, and would contribute to the total variance. By fitting all the data including the four marked data points, a pair of $V_{i\text{-opt}}$ and $PV_{\text{bt-opt}}$ can be obtained. And, by fitting the data excluding the four marked data points, a different pair of $V_{i\text{-opt}}$ and $PV_{\text{bt-opt}}$ can be obtained. In order to identify whether these four data significantly affect the final results or not, comparison is made between the two pairs. If significant difference exists, more experiments with the same flow rates need to be conducted to verify these deviated points and update this curve. **Table 4.1** shows the comparison results with and without the four points.

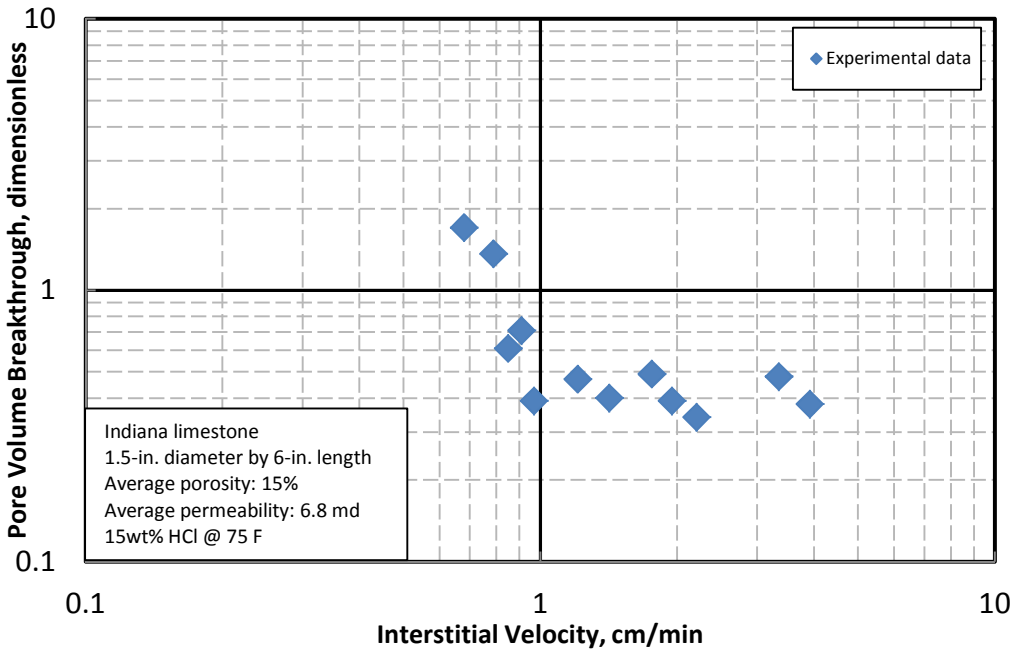

Fig. 4.4—Experimental data for 1.5-in. diameter by 6-in. length cores

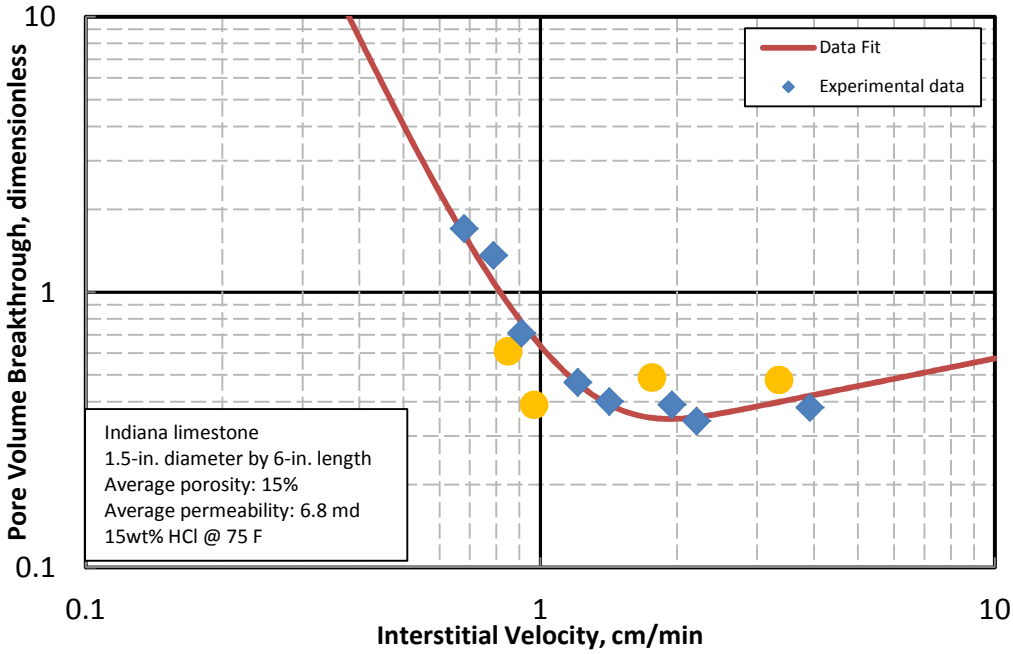

Fig. 4.5—Experimental data and curve fitting for 1.5-in. diameter by 6-in. length cores

Table 4.1 Comparison of $V_{i\text{-opt}}$ and $PV_{\text{bt-opt}}$ for 1.5-in. diameter by 6-in. length cores

	$V_{i\text{-opt}}$, cm/min	$PV_{\text{bt-opt}}$, dimensionless
With the four points	1.96	0.33
Without the four points	2.00	0.33

The results show there is 2% difference for the $V_{i\text{-opt}}$ with and without these four points, which is acceptable.

4.2 Injection Rate Selection

For each group of experiment, the acid injection rate should be selected reasonably. The flow rates should cover three different flow regions, the compact dissolution region, the wormholing region and the branched region. The compact dissolution region is resulted from the low acid injection rate; the wormholing region is resulted from the medium acid injection rate and the branched region is resulted from high acid injection rate.

Darcy's law can be used to calculate the highest injection rate. The syringe pump can supply maximum 2,000 psi pressure, while the backpressure is fixed to 1,000 psi, and therefore the maximum pressure drop across the core is 1,000 psi. The maximum injection rate is related to the maximum pressure drop. With the core dimension and fluid viscosity provided, by measuring the rock permeability beforehand, the maximum flow rate can be calculated.

The flow rate for the experiment should be lower than the maximum flow rate. After three data points are obtained, fit these three data points using Buijse and Glasbergen's model, and a fitting curve will be generated. The three flow regions can be identified from this curve. Select flow rates that lie in these three regions and update this fitting curve. Finally make sure each flow region contains three data points as shown in Fig. 4.3.

Fig. 4.6, **Fig. 4.7** and **Fig. 4.8** show three different typical pressure difference curves with time for three different flow rates in the three regions respectively.

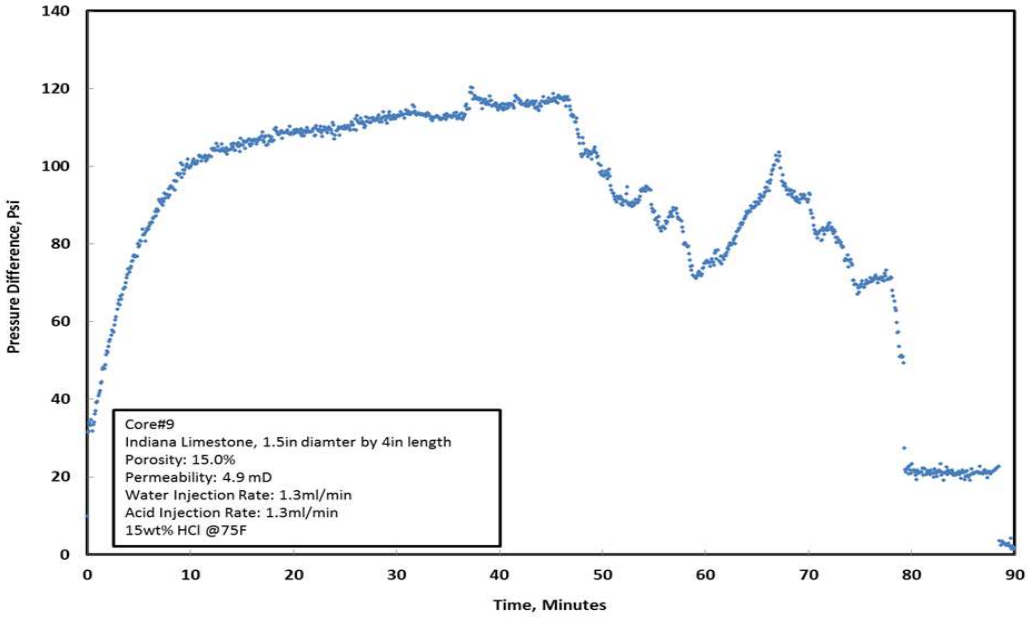

Fig. 4.6(a)—Pressure difference curve under low injection rate

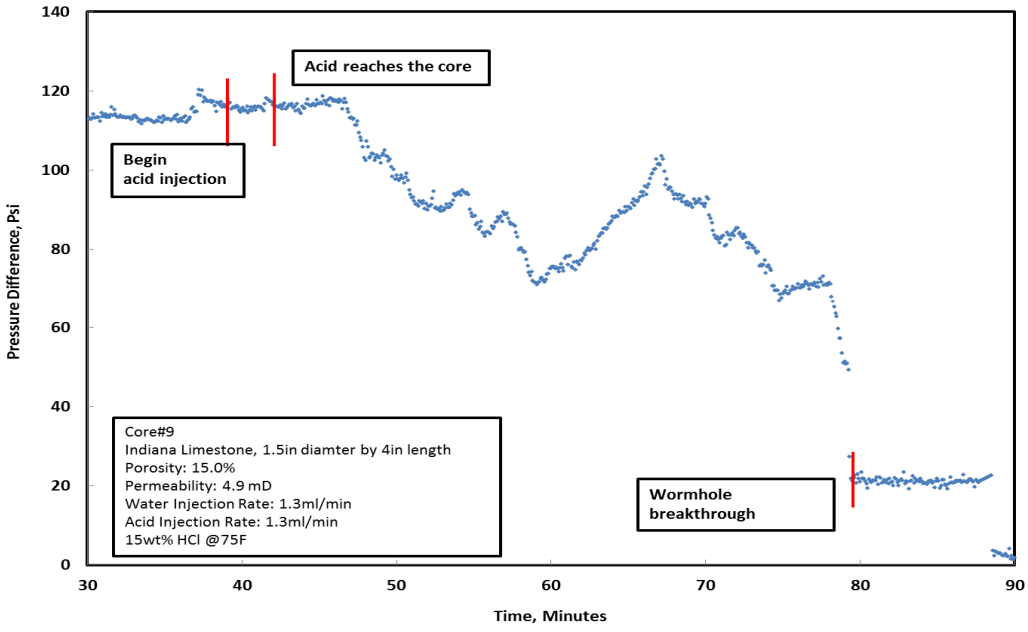

Fig. 4.6(b)—Pressure difference curve during acid injection under low injection rate

Fig. 4.6 shows the pressure drop curve under very low injection rate. The pore volume for wormholes breakthrough is above one. The pressure drop after the acid injection begins is not stable. This is due to the undissolved carbon dioxide created by such low acid injection rate. The backpressure for this experiment is 1,500 psi. Higher backpressure can be tried if the setup can support. For every group of experiment, the pore volume breakthrough above one is necessary for the curve fitting, because it influences the curve position significantly. Two such points are suggested.

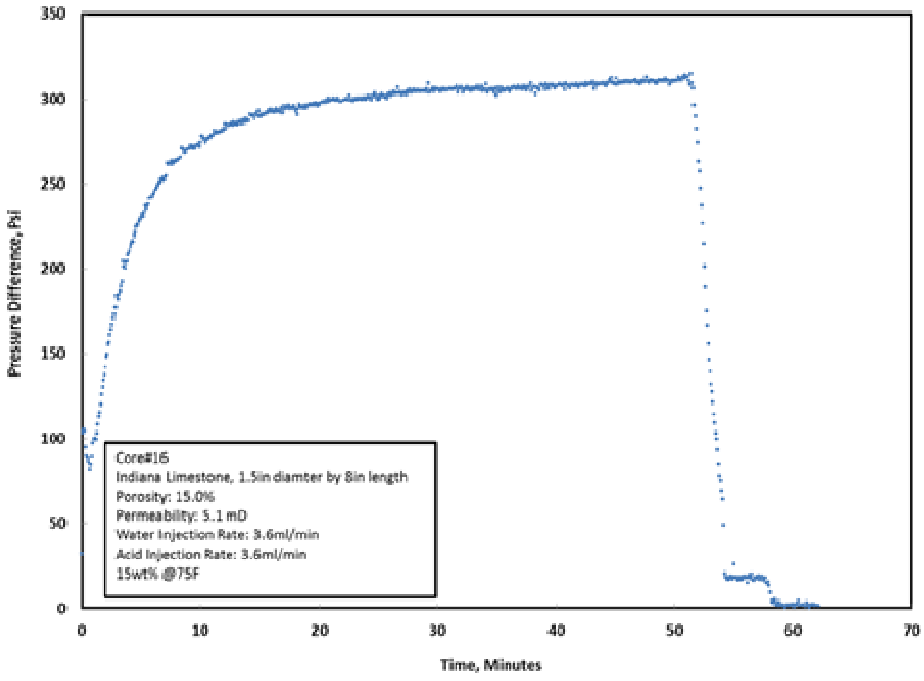

Fig. 4.7(a)—Pressure difference curve under optimum injection rate

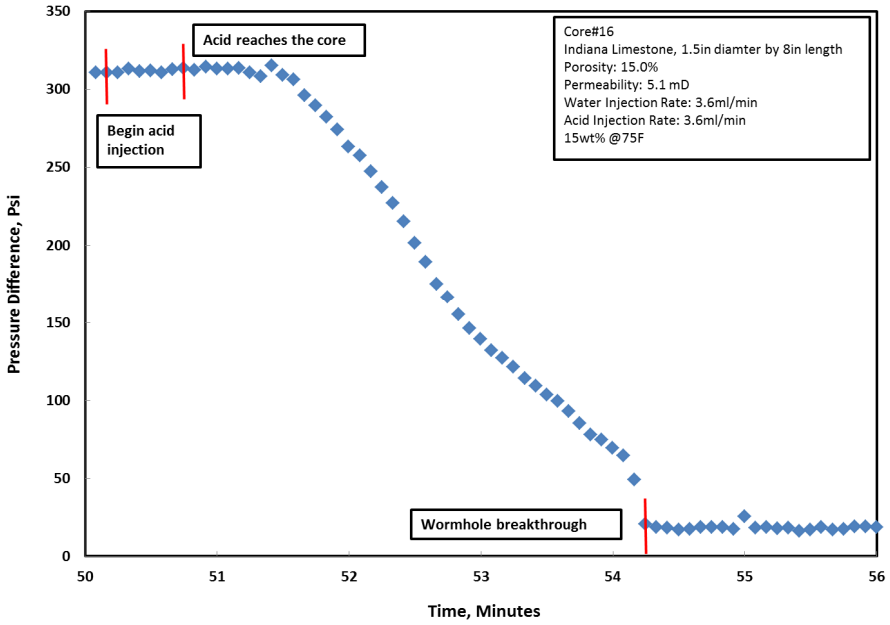

Fig. 4.7(b)—Pressure difference curve during acid injection under optimum injection rate

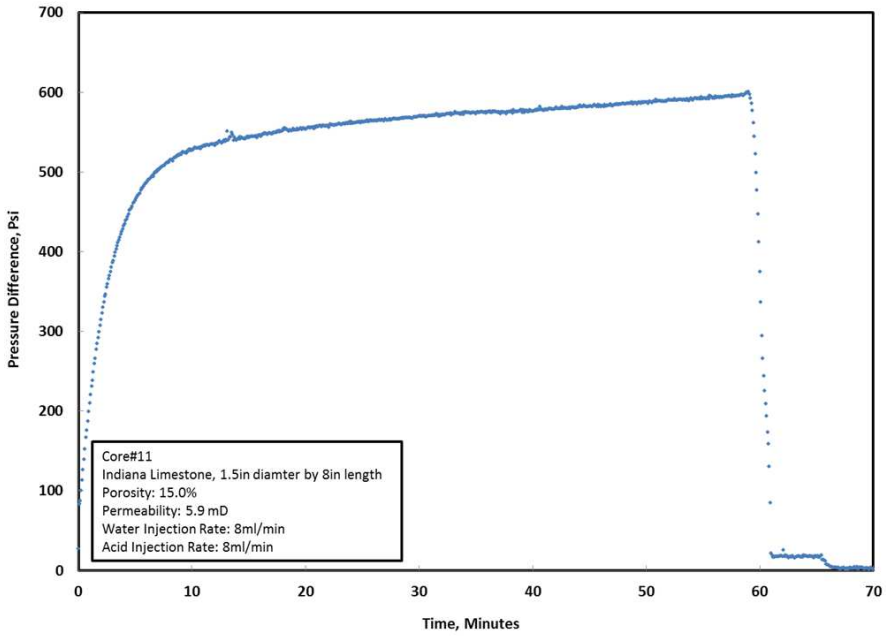

Fig. 4.8(a)—Pressure difference curve under high injection rate

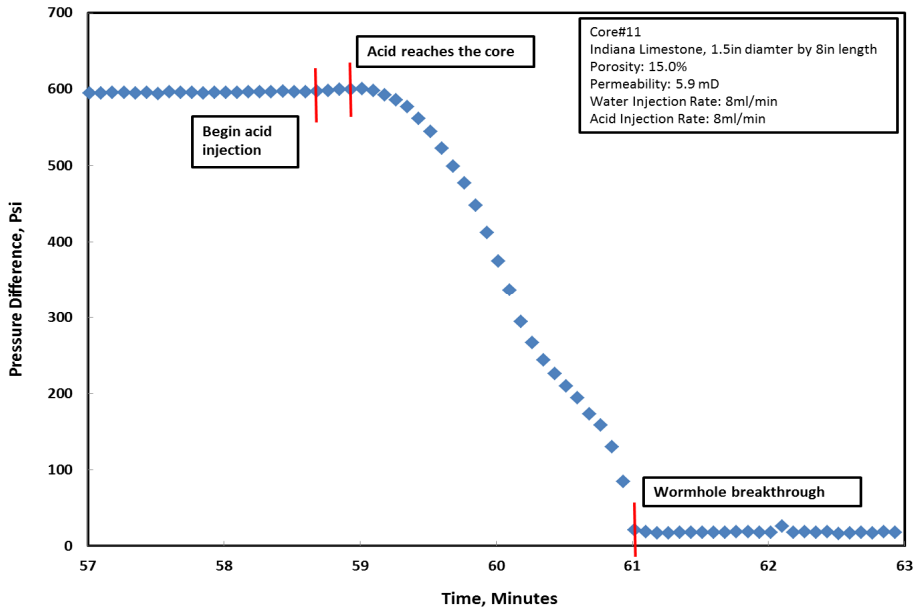

Fig. 4.8(b)—Pressure difference curve during acid injection under high injection rate

The data creates by the optimum injection rate lies in the middle region of the curve shown in Fig. 4.3 while the data of high injection rate lies in the right region of the curve.

Based on the method above, a group of experiments may be completed after 10 individual experiments. Thus, the optimum acid injection rate for this specific group of cores can be calculated by fitting these experimental data. Till now, one optimum acid interstitial velocity is obtained.

Repeat the same experiment for other groups of cores. For each series, four optimum values are obtained for analysis.

4.3 Results for 1-in. Diameter Cores

Four group experiments are conducted for 1-in. diameter cores with four different lengths. The four lengths are 1-in., 2-in., 4-in. and 6-in. **Fig. 4.9-4.12** show the PV_{bt} with V_i for each group of experiments. Fig. 4.9 shows the result for 1-in. length core. It is noticed that the optimal condition did not show clearly. This could be resulted from the short length of the core samples.

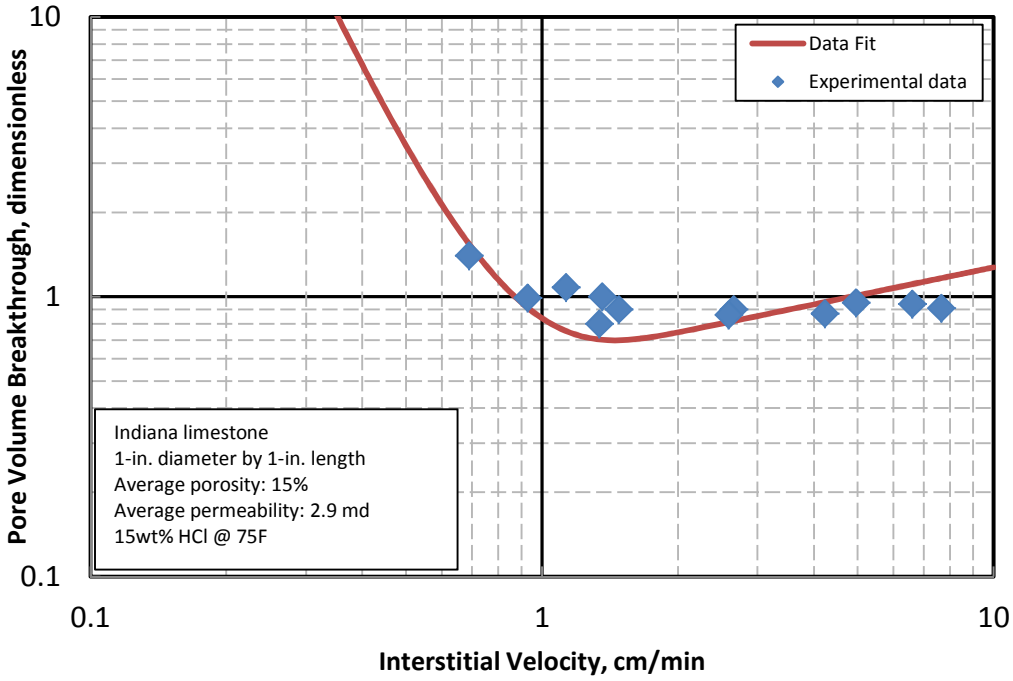

Fig. 4.9—Curve fitting for 1-in. diameter by 1-in. length cores

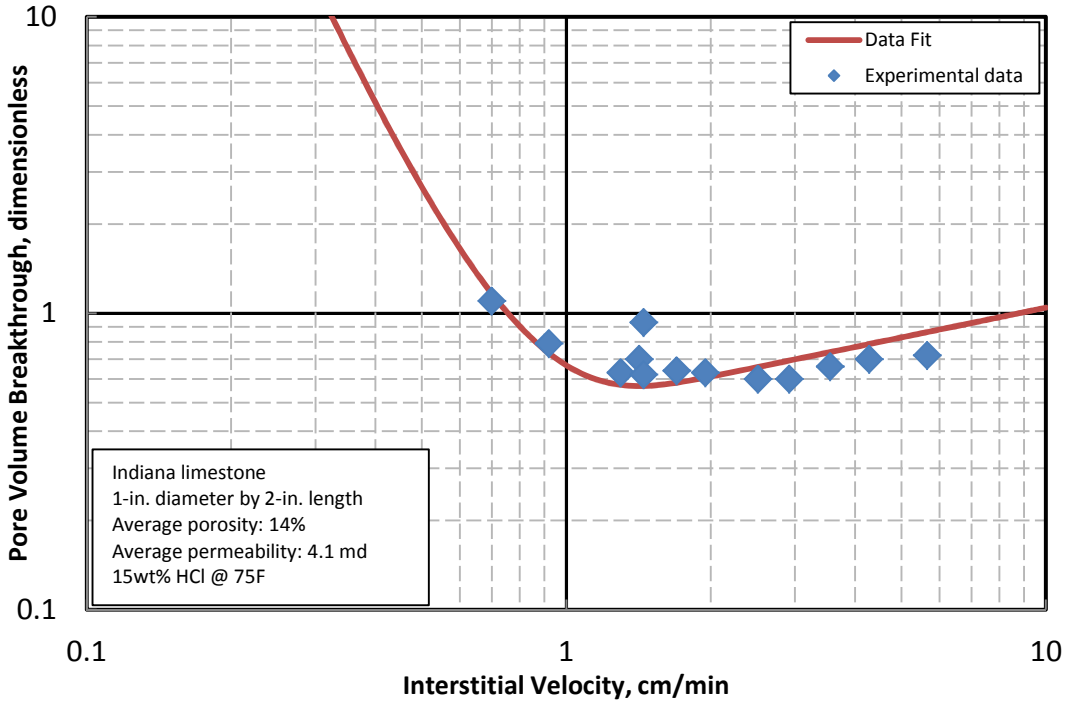

Fig. 4.10—Curve fitting for 1-in. diameter by 2-in. length cores

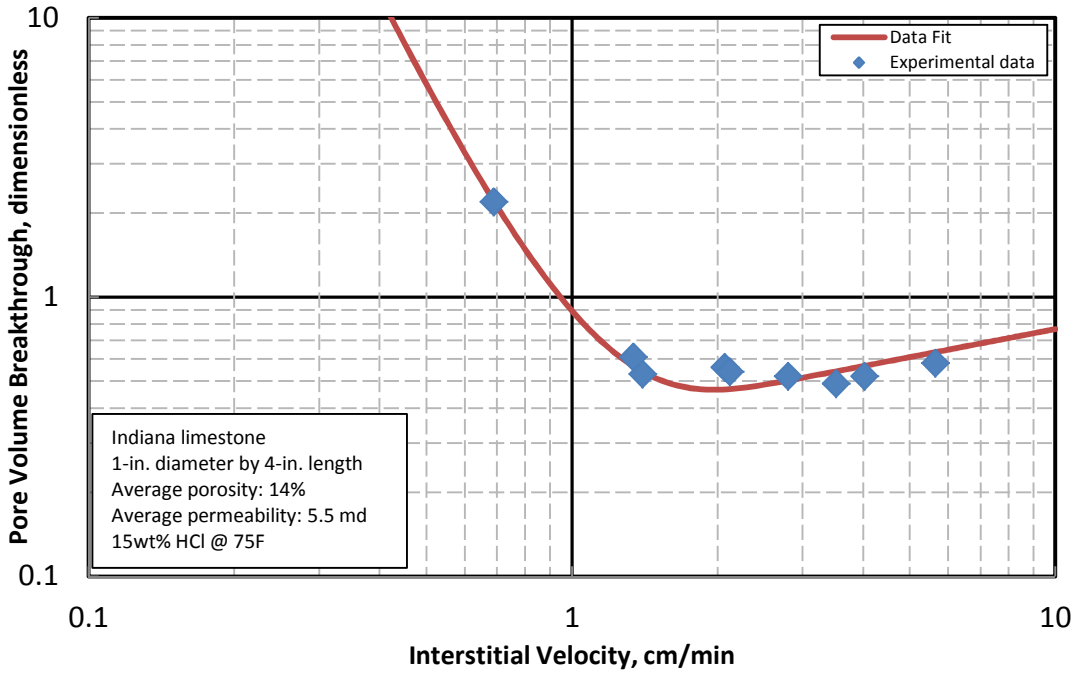

Fig. 4.11—Curve fitting for 1-in. diameter by 4-in. length cores

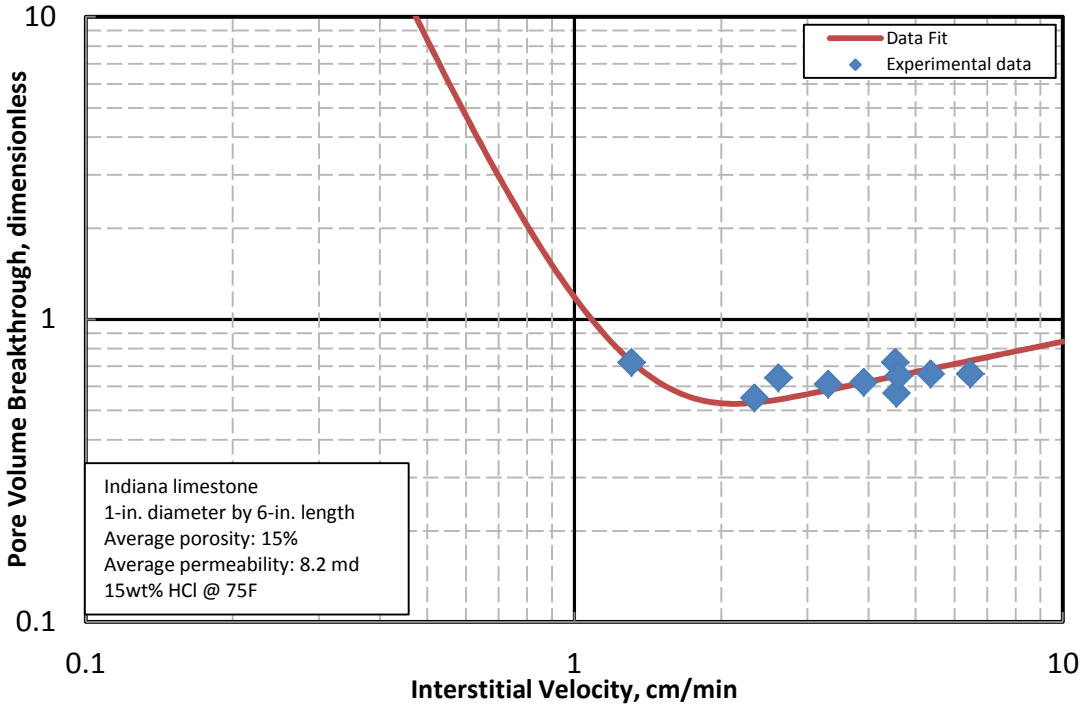

Fig. 4.12—Curve fitting for 1-in. diameter by 6-in. length cores

Fig. 4.13 shows the all four groups of experiments plotted together.

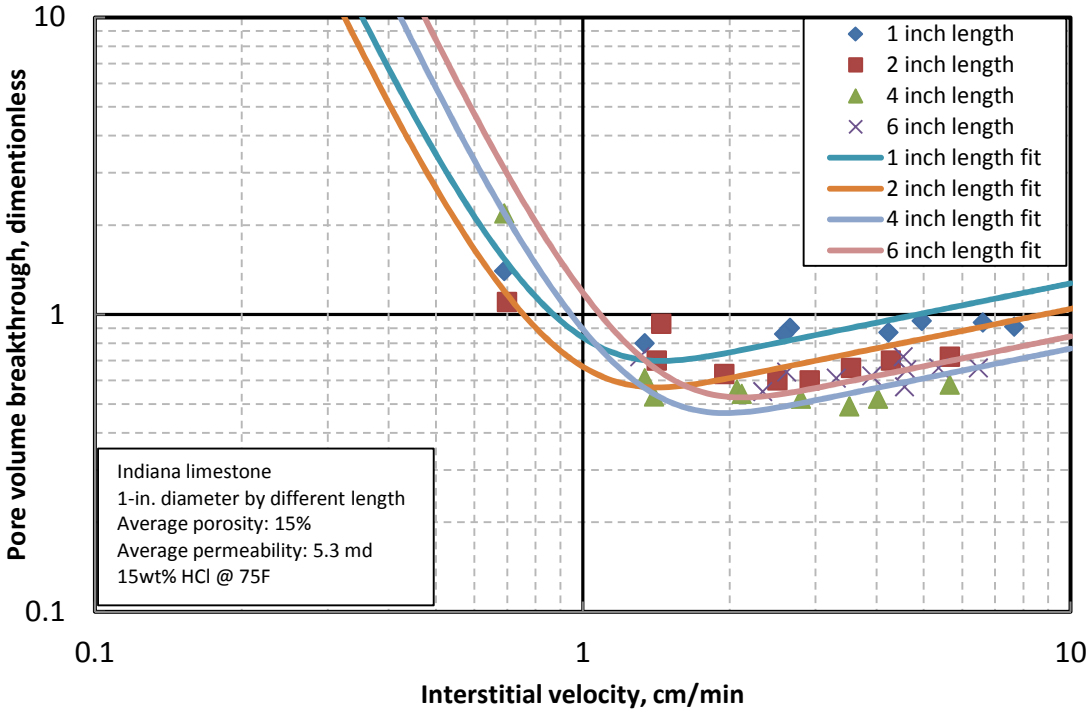

Fig. 4.13—Curve fitting for 1-in. diameter series

Table 4.2 shows the experimental results for 1-in. diameter cores. The average porosity is the average value of all the cores within each group of experiments. So does the average permeability. The optimum acid interstitial velocity and the corresponding optimum pore volume breakthrough are calculated based on Buijse and Glasbergen's model. The residue is a summation of the square of the difference between the experimental data and theoretical value calculated by Eq.4.9.

Table 4.2 Results of 1-in. diameter cores

Length, in.	Amounts of experimetns	Average porosity	Average permeability, md	$V_{i\text{-opt}}$, cm/min	$PV_{\text{bt-opt}}$	Residue
1	12	15%	2.9	1.4763	0.6732	0.38488
2	13	14%	4.3	1.4465	0.5483	0.21117
4	9	14%	5.5	2.0003	0.4493	0.02419
6	10	15%	7.9	2.1631	0.5068	0.02758

The variance for 1-in. length core and 2-in. length core are one-order of magnitude higher than the 4-in. length core and 6-in. length core. With short core length, it is possible that the dominant wormhole has not developed. Increasing the core length provide closer condition to the field. At the outlet, 1-in. length core shows several small wormholes as shown in **Fig. 4.14**.

Fig. 4.14—Outlet surface of the 1-in. diameter by 1-in. length core

Fig. 4.15 shows the optimum acid injection rate against the core length.

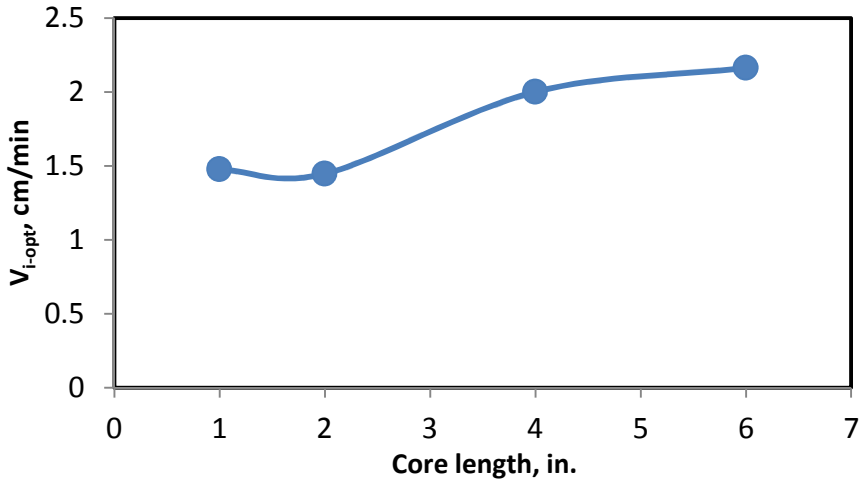

Fig. 4.15—$V_{i\text{-opt}}$ for 4 different core lengths with 1-in. diameter

It seems the curve is still going up if the results of longer cores are available. The $V_{i\text{-opt}}$ for 1-in. length core and 2-in. length core are almost the same. However, Bazin (2001) found the optimum injection rate increases with the increasing of the core length. For the length of 2 in., 4 in. and 6 in., it shows agreement with this statement. Together with the multiple holes on the outlet surface of 1-in. length cores, we can conclude that 1-in length core is not suitable to find the optimum value in matrix acidizing experiment.

6-in. is the maximum length that the 1-in. diameter core holder can support. The $V_{i\text{-opt}}$ is still dependent on the core length. Therefore, 1.5-in. diameter cores should be used for further investigation.

4.4 Results for 1.5-in. Diameter Cores

Four groups of experiments are conducted for 1.5-in. diameter cores. The four lengths are 4 in., 6 in., 8 in. and 10 in. **Figs. 4.16-4.19** show the PV_{bt} with V_i for each group of experiments.

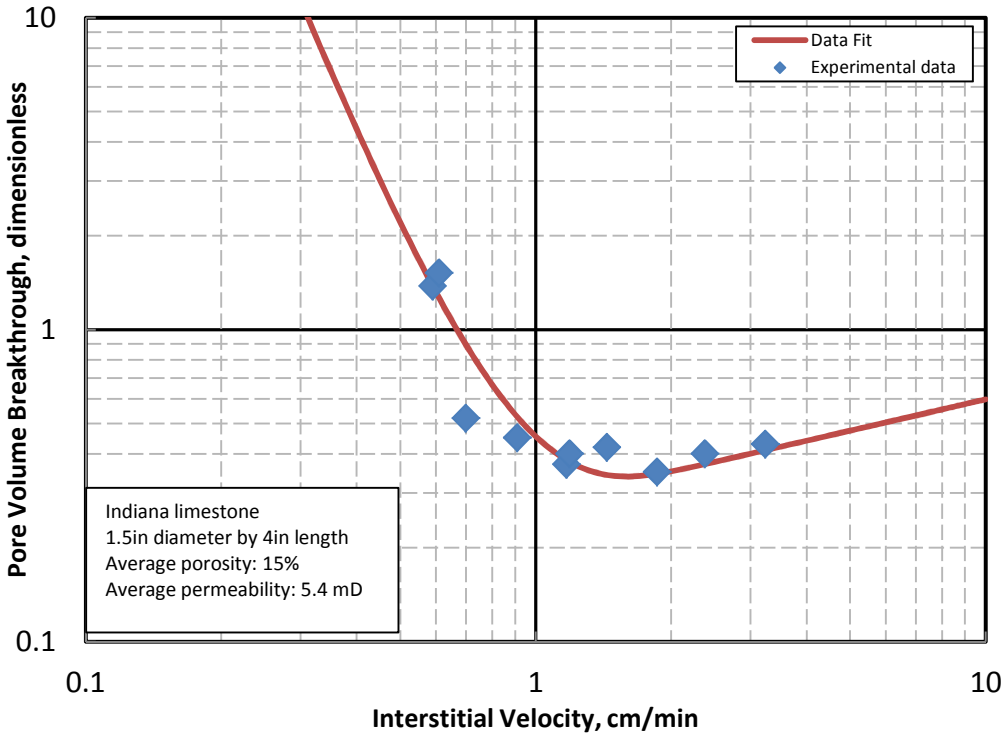

Fig. 4.16—Curve fitting for 1.5-in. diameter by 4-in. length cores

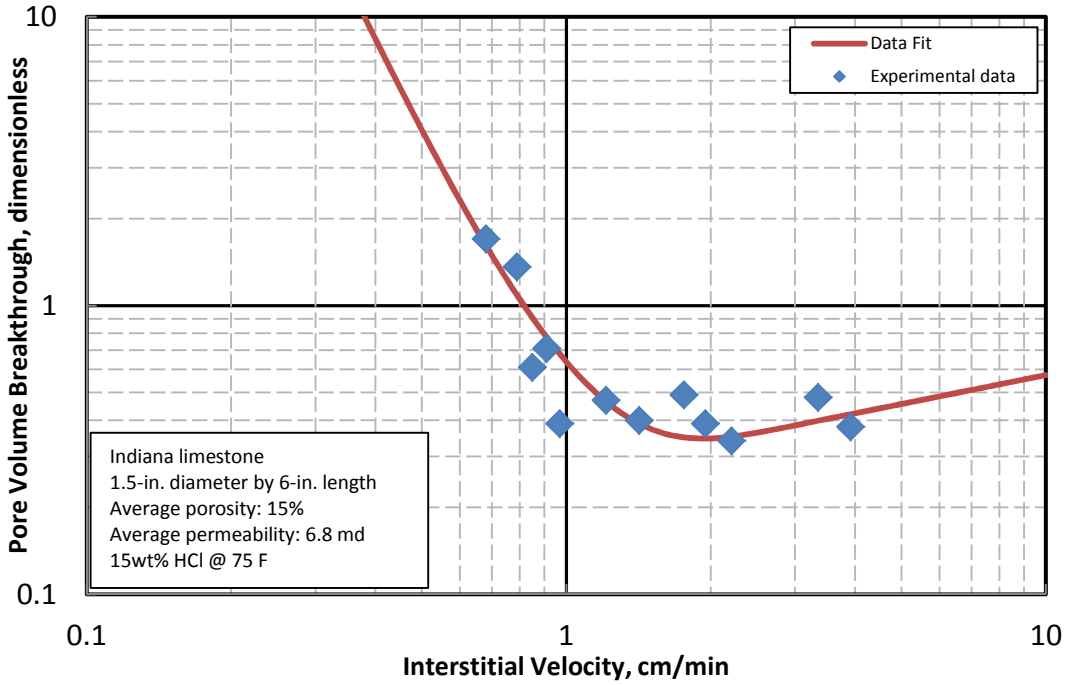

Fig. 4.17—Curve fitting for 1.5-in. diameter by 6-in. length cores

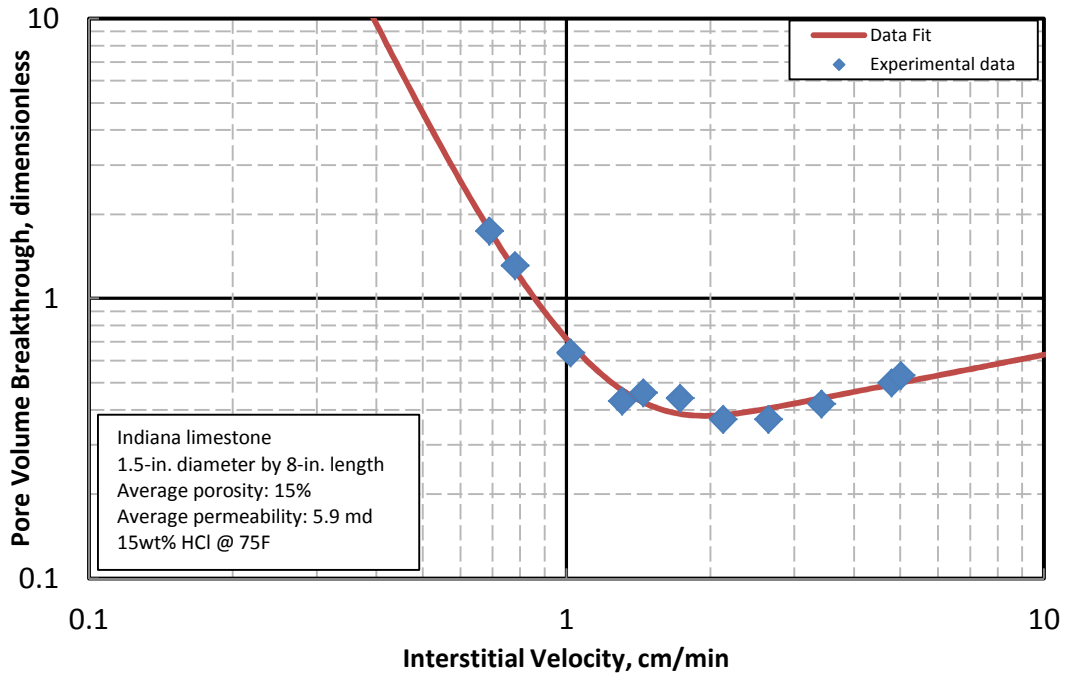

Fig. 4.18—Curve fitting for 1.5-in. diameter by 8-in. length cores

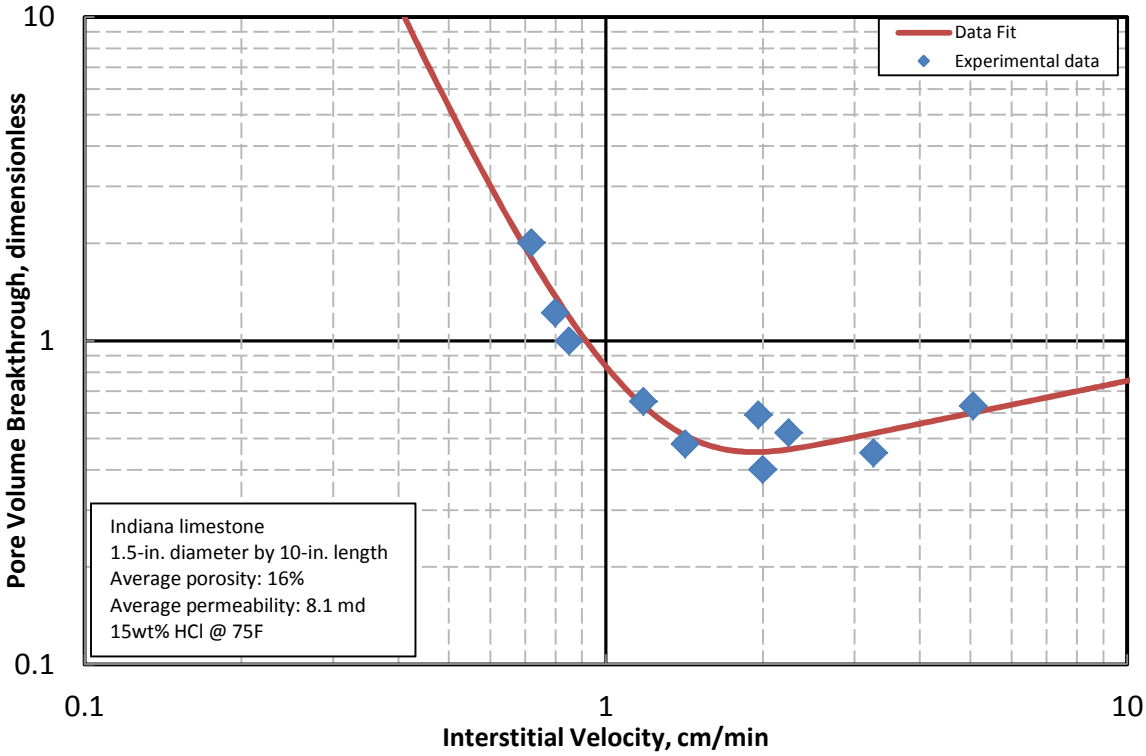

Fig. 4.19—Curve fitting for 1.5-in. diameter by 10-in. length cores

Fig. 4.20 shows the all four sets of experiments plotted together. It can be seen that the transition points for 6-in., 8-in. and 10-in. length corresponds to the same V_i but different PV_{bt}. The results are summarized in **Table 4.3**.

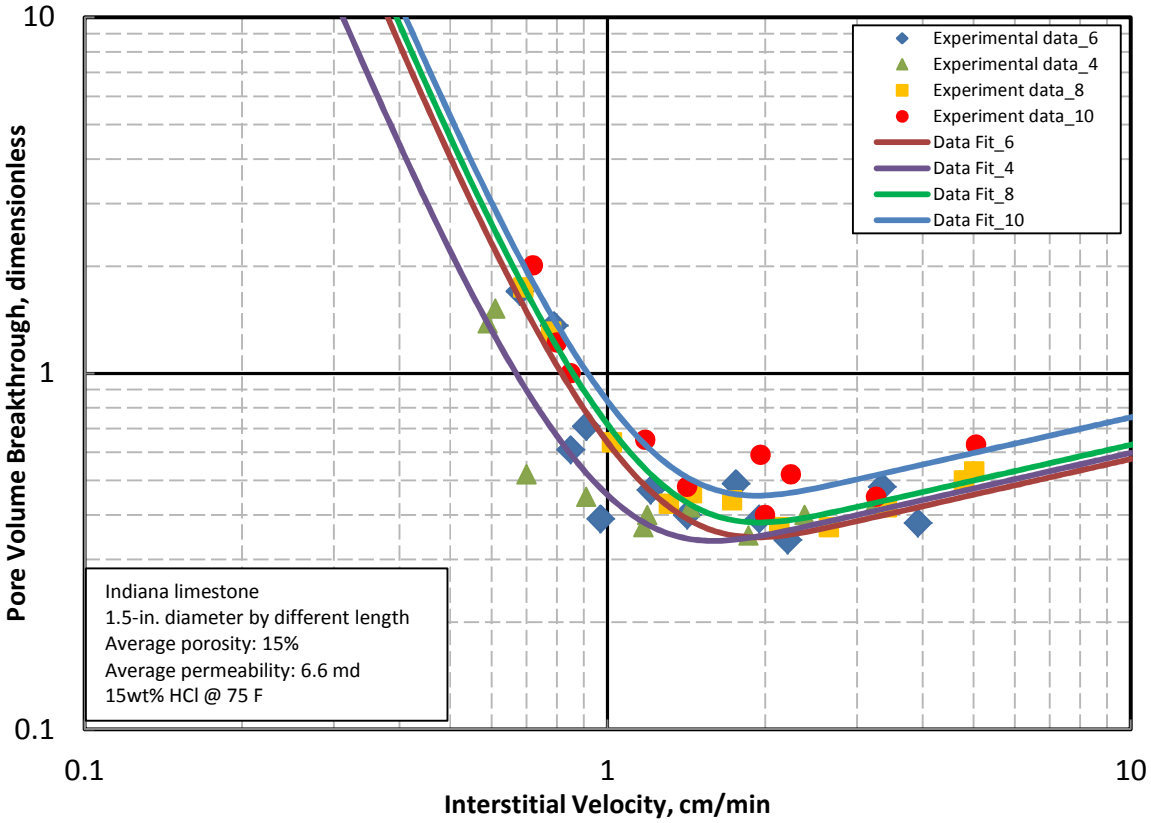

Fig. 4.20—Curve fitting for 1.5-in. diameter cores series

Table 4.3 shows the results of 1.5-in. diameter cores.

Table 4.3 Results of 1.5-in. diameter cores

Length, in.	Amounts	Average porosity	Average permeability, md	$V_{i\text{-opt}}$, cm/min	$PV_{\text{bt-opt}}$	Variance
4	11	15%	5.4	1.6228	0.3262	0.21997
6	12	15%	6.8	1.9630	0.3340	0.29015
8	11	15%	5.9	1.9837	0.3674	0.01317
10	10	16%	8.1	1.9600	0.4371	0.13243

Fig. 4.21 shows the $V_{i\text{-opt}}$ for the 4 different core lengths with 1.5-in. diameter cores. There is an increase of the $V_{i\text{-opt}}$ from 4-in. core length to 6-in. core length. And the $V_{i\text{-opt}}$ almost remain the same from 6-in. length to 10-in. length, which indicates that if the core is longer than 6 in., the $V_{i\text{-opt}}$ is independent of the core length.

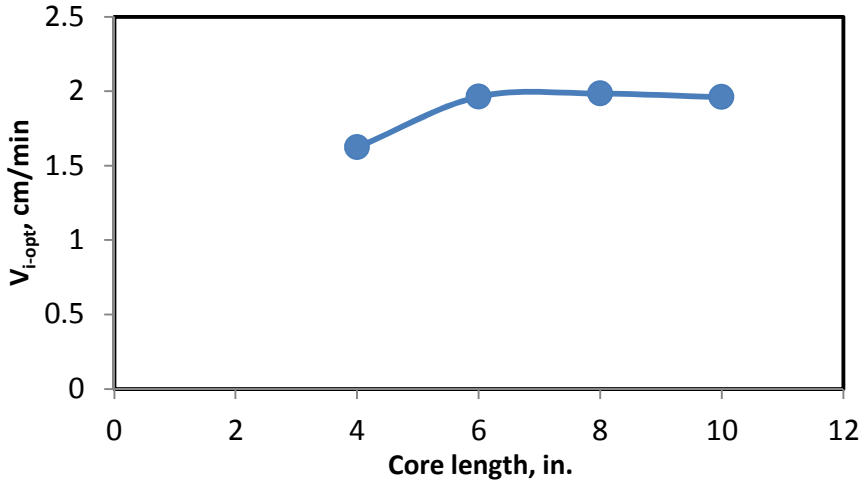

Fig. 4.21—$V_{i\text{-opt}}$ for 4 different core lengths with 1.5-in. diameter

4.5 Summary

In this section, we discussed how to get the optimum acid interstitial velocity from the experimental data. Eight groups of experiments are conducted, leading to eight optimum acid interstitial velocities. We have found that when the core reaches a certain length, the $V_{i\text{-opt}}$ is independent of the core length.

5. CONCLUSION & RECOMMENDATION

In this research, two series of experiments with two different diameters for each series have been conducted to study the effect of the core length on the optimal condition of wormhole growth. Each series contains four groups of experiments with four different core lengths respectively. The optimum acid interstitial velocity for each group is obtained and the following conclusions can be made.

- The optimum acid injection rate depends on the core length.
- With the core length increasing, the optimum acid injection rate increases.
- When the core length reaches a certain value, the optimum acid injection rate is independent of the core length.

Further work can be done for this research. The recommendations for future work are listed below.

- The core diameter effect can be investigated by doing experiments with 4-in diameter cores.
- The influence of acid concentration, temperature on the optimum acid injection rate needs to be identified.
- Comprehensive correlation can be developed to predict the optimum acid injection rate under a certain reservoir conditions.

REFERENCES

Bazin, B. 2001. From Matrix Acidizing to Acid Fracturing: A Laboratory Evaluation of Acid/Rock Interactions. *SPE Production & Facilities* **16** (1): 22-29.

Buijse, M.A. 2000. Understanding Wormholing Mechanisms Can Improve Acid Treatments in Carbonate Formations. *SPE Production & Operations* **15** (3): 168-175. doi: 10.2118/65068-pa

Buijse, M.A. and Glasbergen, G. 2005. A Semiempirical Model to Calculate Wormhole Growth in Carbonate Acidizing. Paper SPE 96892 presented at the SPE Annual Technical Conference and Exhibition, Dallas, Texas, 10/09/2005. doi: 10.2118/96892-ms

Daccord, G. 1987. Chemical Dissolution of a Porous Medium by a Reactive Fluid. *Physical Review Letters* **58** (5): 479-482.

Daccord, G., Nittmann, J., and Stanley, H.E. 1986. Radial Viscous Fingers and Diffusion-Limited Aggregation: Fractal Dimension and Growth Sites. *Physical Review Letters* **56** (4): 336-339.

Daccord, G., Touboul, E., and Lenormand, R. 1989. Carbonate Acidizing: Toward a Quantitative Model of the Wormholing Phenomenon. *SPE Production Engineering* **4** (1): 63-68. doi: 10.2118/16887-pa

DRESSER, Inc. 2012. Mity Mite back pressure regulator. http://www.dresser.com/documents/RedQ/regulator_broc_redq_spec_reg_brochure_f.pdf. Downloaded 14 April 2012

Fredd, C.N. and Fogler, H.S. 1999. Optimum Conditions for Wormhole Formation in Carbonate Porous Media: Influence of Transport and Reaction. *SPE Journal* **4** (3): 196-205. doi: 10.2118/56995-pa

Frick, T.P., Mostofizadeh, B., and Economides, M.J. 1994. Analysis of Radial Core Experiments for Hydrochloric Acid Interaction with Limestones. Paper Copyright 1994, SPE 27402 presented at the SPE Formation Damage Control Symposium, Lafayette, Louisiana, 02/07/1994. doi: 10.2118/27402-ms

Furui, K., Burton, R.C., Burkhead, D.W., Abdelmalek, N.A., Hill, A.D. et al. 2010. A Comprehensive Model of High-Rate Matrix Acid Stimulation for Long Horizontal Wells in Carbonate Reservoirs. Paper SPE 134265-MS presented at the SPE Annual Technical Conference and Exhibition, Florence, Italy, 09/19/2010. doi: 10.2118/134265-ms

Gdanski, R. 1999. A Fundamentally New Model of Acid Wormholing in Carbonates. Paper SPE 54719 presented at the SPE European Formation Damage Conference, The Hague, Netherlands, 05/31/1999. doi: 10.2118/54719-ms

Glasbergen, G., Kalia, N., and Talbot, M.S. 2009. The Optimum Injection Rate for Wormhole Propagation: Myth or Reality? Paper SPE 121464 presented at the 8th European Formation Damage Conference, Scheveningen, The Netherlands, 05/27/2009. doi: 10.2118/121464-ms

Guin, J.A. and Schechter, R.S. 1971. Matrix Acidization with Highly Reactive Acids. *Society of Petroleum Engineers Journal* **11** (4): 390-398. doi: 10.2118/3091-pa

Guin, J.A., Schechter, R.S., and Silberberg, I.H. 1971. Chemically Induced Changes in Porous Media. *Industrial & Engineering Chemistry Fundamentals* **10** (1): 50-54. doi: 10.1021/i160037a010

Hoefner, M.L. and Fogler, H.S. 1987. Role of Acid Diffusion in Matrix Acidizing of Carbonates. *SPE Journal of Petroleum Technology* **39** (2): 203-208. doi: 10.2118/13564-pa

Hoefner, M.L. and Fogler, H.S. 1988. Pore Evolution and Channel Formation During Flow and Reaction in Porous Media. *AIChE Journal* **34** (1): 45-54. doi: 10.1002/aic.690340107

Hoefner, M.L. and Fogler, H.S. 1989. Fluid-Velocity and Reaction-Rate Effects During Carbonate Acidizing: Application of Network Model. *SPE Production Engineering* **4** (1): 56-62. doi: 10.2118/15573-pa

Huang, T., Hill, A.D., and Schechter, R.S. 2000. Reaction Rate and Fluid Loss: The Keys to Wormhole Initiation and Propagation in Carbonate Acidizing. *SPE Journal* **5** (3): 287-292. doi: 10.2118/65400-pa

Huang, T., Zhu, D., and Hill, A.D. 1999. Prediction of Wormhole Population Density in Carbonate Matrix Acidizing. Paper SPE 54723 presented at the SPE European Formation Damage Conference, The Hague, Netherlands, 05/31/1999. doi: 10.2118/54723-ms

Hung, K.M., Hill, A.D., and Sepehrnoori, K. 1989. A Mechanistic Model of Wormhole Growth in Carbonate Matrix Acidizing and Acid Fracturing. *SPE Journal of Petroleum Technology* **41** (1). doi: 10.2118/16886-pa

Mcduff, D., Shuchart, C.E., Jackson, S., Postl, D., Brown, J.S. et al. 2010. Understanding Wormholes in Carbonates: Unprecedented Experimental Scale and 3-D Visualization. Paper SPE 134379 presented at the SPE Annual

Technical Conference and Exhibition, Florence, Italy, 09/19/2010. doi: 10.2118/134379-ms

Michael J. Economides, A. Daniel Hill, Christine Ehlig-Economides, C.: *Petroleum Production System*, 400. 1993. Upper Saddle River, New Jersey: Prentice Hall, Inc.

Mostofizadeh, B. and Economides, M.J. 1994. Optimum Injection Rate from Radial Acidizing Experiments. Paper SPE 28547 presented at the SPE Annual Technical Conference and Exhibition, New Orleans, Louisiana, 09/25/1994. doi: 10.2118/28547-ms

Nittmann, J., Daccord, G., and Stanley, H.E. 1985. Fractal Growth Viscous Fingers: Quantitative Characterization of a Fluid Instability Phenomenon. *Nature* **314** (6007): 141-144.

Pichler, T., Frick, T.P., Economides, M.J., and Johann, N. 1992. Stochastic Modeling of Wormhole Growth in Carbonate Acidizing with Biased Randomness. Paper SPE 25004 presented at the European Petroleum Conference, Cannes, France, 11/16/1992. doi: 10.2118/25004-ms

Schechter, R.S. and Gidley, J.L. 1969. The Change in Pore Size Distribution from Surface Reactions in Porous Media. *AIChE Journal* **15** (3): 339-350. doi: 10.1002/aic.690150309

Talbot, M.S. and Gdanski, R.D. 2008. Beyond the Damkohler Number: A New Interpretation of Carbonate Wormholing. Paper SPE 113042 presented at the Europec/EAGE Conference and Exhibition, Rome, Italy, 06/09/2008. doi: 10.2118/113042-ms

Teledyne Isco, Inc. 2012. D Series Pump http://www.isco.com/products/products3.asp?PL=1051010. Downloaded 14 April 2012

Wang, Y., Hill, A.D., and Schechter, R.S. 1993. The Optimum Injection Rate for Matrix Acidizing of Carbonate Formations. Paper SPE 26578 presented at the SPE Annual Technical Conference and Exhibition, Houston, Texas, 10/03/1993. doi: 10.2118/26578-ms

APPENDIX

Procedure for starting Labview

1. Double click the Labview icon, the Labview main interface appears shown in **Fig. 1**

Fig. 1—Labview main interface

2. In the Open column, several .vi files show up with one named ACIDIZING calibrated in winter2011.vi. Click it and then the VI file interface will show up, like in **Fig. 2**. There are three charts for dynamic monitoring, with the upper one for permeability and the other two for pressure difference.

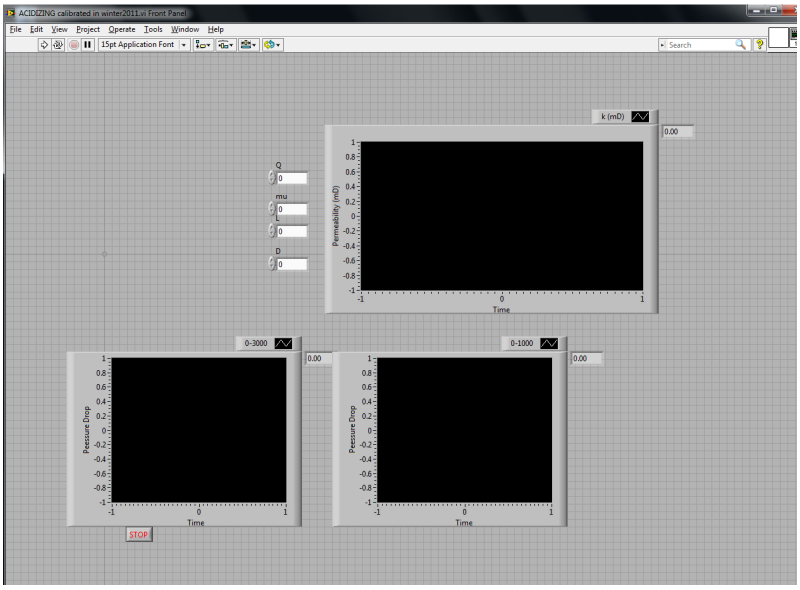

Fig. 2—VI file interface

3. Double click any of the chart, the diagram for this VI file will show up as in **Fig. 3**. This diagram describes the working principle of this VI file.

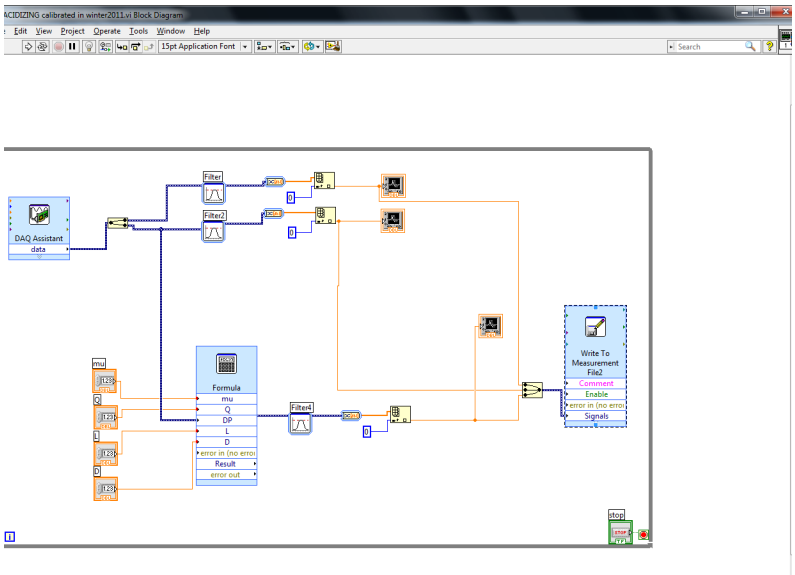

Fig. 3—Diagram of VI file

4. Double click Write To Measurement File module. It will lead to the interface for specifying file directory as shown in **Fig. 4**.

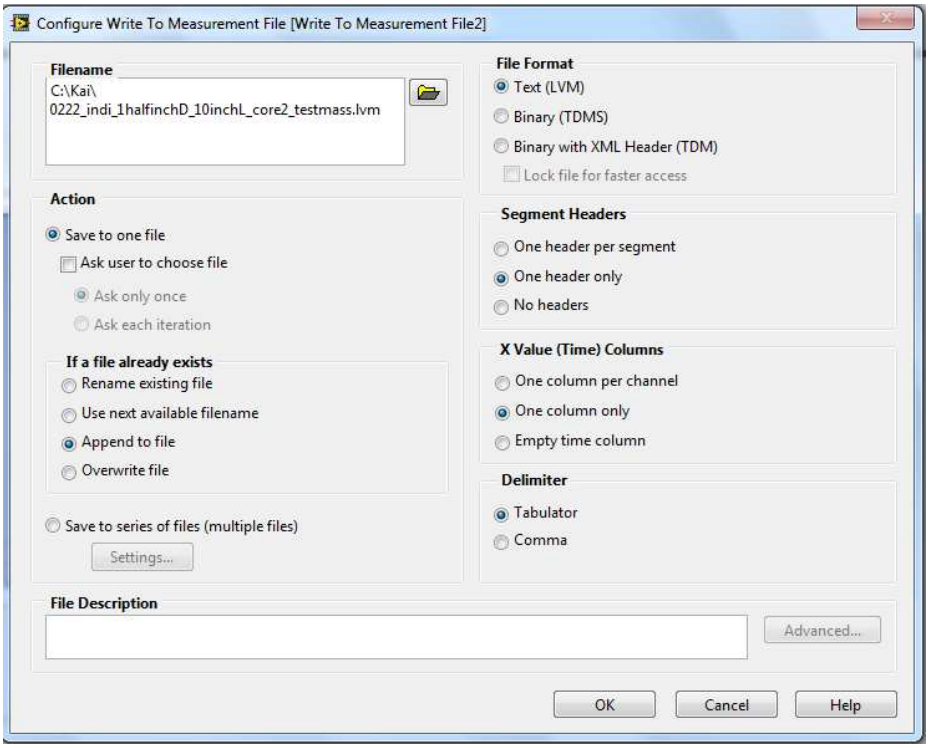

Fig. 4—Specifying file directory

5. Click the Folder Icon, specify the file directory and then click OK. It will then lead to the VI interface as shown in Fig. 2. Till now, the VI file is ready to run. If click the Run icon, the Labview will begin to read the signal transefered from the pressure transducer, and the pressure drop data will show up in the chart with time.

VITA

Name:	Kai Dong
Address:	714 Richardson Building, 3116 TAMU, College Station, TX 77843-3116
Email Address:	dongkai.tamu@gmail.com
Education:	B.S., Petroleum Engineering, China University of Petroleum Beijing, 2009 M.S., Petroleum Engineering, Texas A&M University, 2012